NASA TN D-1502

TECHNICAL NOTE

D-1502

NOISE MEASUREMENTS DURING CAPTIVE AND LAUNCH FIRINGS OF A LARGE ROCKET-POWERED VEHICLE

By William H. Mayes and Philip M. Edge, Jr.

Langley Research Center
Langley Station, Hampton, Va.

NATIONAL AERONAUTICS AND SPACE ADMINISTRATION
WASHINGTON
November 1962

NATIONAL AERONAUTICS AND SPACE ADMINISTRATION

TECHNICAL NOTE D-1502

NOISE MEASUREMENTS DURING CAPTIVE AND LAUNCH FIRINGS OF A LARGE ROCKET-POWERED VEHICLE

By William H. Mayes and Philip M. Edge, Jr.

SUMMARY

Noise levels and spectra are presented for captive and launch firings of a large rocket-powered (Atlas) vehicle. Included are measurements made while the vehicle exhaust was deflected 90° by a water-cooled turning bucket as well as when the exhaust was free of the bucket deflector. Data were obtained along the vehicle itself and at ground stations for a distance of 3,500 feet from the vehicle.

Noise levels along the length of the vehicle varied from 144 db at the payload to 154 db near the nozzle exit. The noise pattern around the vehicle was unsymmetrical while the exhaust deflector was in use. For short periods of time during the ignition and burnout, the measured sound-pressure-level values in the near field were about 10 to 15 db higher than those measured for the rated thrust condition. During launch, noise levels varied from 170 db at a station close to the vehicle to 116 db at a station 3,500 feet from the vehicle. Sound pressure levels above a given value persist longer at locations close to the launch site than at greater distances. Radiation patterns obtained during the moving phase of launch were found to agree with Scout vehicle data adjusted to similar operating conditions.

INTRODUCTION

The intense noise generated by rocket engines in the ground launching of large missiles and space vehicles is of concern because of possible detrimental effects on the vehicle itself and the supporting equipment and personnel near the launch site. It is known that intense noise can cause malfunction of sensitive equipment, damage to vehicle structures and to ground building structures, interference with communications, and annoyance to people. Inasmuch as space exploration programs demand rocket engines having greater thrust, the associated noise generated becomes of increasing concern. Thus, there is a need for a detailed understanding of the intense noise generated by present-day large rocket engines and for the prediction of the noise of larger rocket engines of the future. To further this understanding and to obtain data on large booster engines, the noise associated with launchings of a large rocket-powered vehicle was measured with a view toward applying these data to the prediction of noise for larger launch vehicles of the future.

Noise survey data for rockets and supersonic jets have been obtained for a range of thrust ratings under varied firing conditions and are presented in references 1 to 7. References 1 and 2 include data for both solid- and liquid-propellant rockets, a thrust range from 1,000 to 130,000 pounds, and conditions of nearly horizontal firings. Reference 3 presents noise surveys for a large supersonic wind-tunnel exhaust jet of 475,000 pounds thrust exhausting horizontally. References 4, 5, and 6 present data for captive firings of rocket engines in the thrust range from 150,000 to 1,000,000 pounds and for conditions of vertical firing with turning buckets used to deflect the exhaust flow. Of particular interest is reference 7 which presents far-field noise survey data for launchings of two Saturn vehicles.

The present paper gives detailed noise-measurement information obtained during the nonmoving and moving phases of the launchings of a large rocket-powered vehicle. This vehicle, with a thrust rating of 360,000 pounds, was captive fired and launched in a vertical position. During captive firing and early stages of lift-off, the rocket exhaust was deflected in a horizontal direction by a water-cooled L-shaped turning bucket. The data were obtained at Cape Canaveral, Florida, during the launching of a Project Mercury type space vehicle. Overall noise levels and noise spectra are presented for stations along and around the launch vehicle during captive firing. Simultaneous launch noise measurements are presented for several stations on the launch complex and on the ground for a distance of 3,500 feet from the launch vehicle. Resulting noise radiation patterns obtained for these two launchings are compared with noise radiation patterns for a Scout launching at the NASA Wallops Station.

SYMBOLS

D_e	equivalent nozzle exit diameter
h	altitude, ft
N	number of crossings associated with a given value of p_{ref}
N_{max}	maximum number of crossings associated with any value of p_{ref}
p_{ref}	arbitrary reference pressure
p_{rms}	root-mean-square pressure
x	horizontal distance measured from launch-vehicle center line, ft
y	vertical distance along launch vehicle measured from nozzle exit plane, ft
α	angle measured from center line of deflected exhaust to measuring station, deg

β angle measured from thrust axis at rear of launch vehicle to measuring station, deg

$\sigma = \frac{p_{ref}}{p_{rms}}$

APPARATUS AND TEST CONDITIONS

Launch Vehicle and Launch Site

Most of the data of this paper were obtained during the captive firing and launch firing of the Atlas 10-D vehicle at Cape Canaveral, Florida (fig. 1). The payload of this launching was a full-scale Project Mercury spacecraft of simplified construction. The three rocket engines of this 85-foot-long Atlas vehicle had a total thrust rating of about 360,000 pounds at lift-off. The vehicle was suspended vertically on the launch pad at a distance of about 25 feet above ground level. The rocket-engine exhaust was directed into an enclosed 90° turning bucket located below the exhaust nozzle in such a manner that the exhaust impinged on the bucket walls at a distance of about 15 feet below the nozzle. Cooling of the turning bucket was accomplished by injection of water into the exhaust through holes in the bucket walls. The exhaust bucket was positioned so that the direction of the deflected exhaust was 15° east of north. The terrain in the immediate area of the launch complex was essentially flat.

Additional data were obtained during the launching of the Atlas 11-C vehicle from an adjacent launch pad located 4,000 feet distant.

Noise Instrumentation

All noise measurements were obtained by use of commercially available condenser microphones and associated preamplifier systems having a usable frequency range from 5 to 10,000 cps. The outputs were recorded on a multichannel FM tape recording system having a usable frequency range from 0 to 10,000 cps.

The microphone locations for both the static firing and the launch firing of the Atlas 10-D vehicle are indicated schematically in figure 2. As noted in figure 2, for the captive firing one microphone was attached to the skin surface of the spacecraft, three microphones were attached to the surface of the launch vehicle in the vicinity of the equipment bays (y = approx. 35 feet), and one microphone was located near the missile skirt section but was not attached to it. It should be noted that some of the microphones were on the same side of the vehicle as the exhaust and some were on the opposite side. Two microphones were attached to the service tower located approximately 23 feet from the vehicle center line, and one microphone was located at a distance of about 500 feet. For the launch firing the five microphones located on or near the vehicle surface were removed and placed in a horizontal straight-line array varying from 50 to 100 feet from the vehicle as indicated in the figure. The tape recorder and associated equipment were located in a van approximately 250 feet from the base of the vehicle, the tape recorder being remotely controlled from the launch-complex blockhouse.

Because of a concern for possible detrimental effects on the measuring and recording equipment, the entire van and associated equipment had been previously proof tested in the noise environment of a large blowdown wind tunnel (ref. 3). To minimize any possible effects of structural acceleration or vibrations, the microphones were shock mounted along the vehicle structure. There was no evidence of microphonics in the system used, either during the environmental proof tests or during the data acquisition. Effects of temperature were minimized by means of thermal insulation around each microphone.

Weather Conditions

Lift-off of the Atlas 10-D vehicle occurred at 2:20 a.m. in clear weather with 10-mile visibility, 0.1 cumulus cloud cover with base at approximately 2,200 feet, and 0.6 altocumulus with base estimated at 10,000 feet. The ambient surface temperature was 74° F, the relative humidity was 97 percent, the dewpoint was 73° F, and surface wind was from the north at 3 knots. From rawinsonde information obtained within 1 hour of launch time, the data on temperature, wind velocity, and wind direction as a function of altitude were obtained. Components of the wind velocity parallel to and perpendicular to the ground microphone array for the altitude range from 0 to 50,000 feet are shown in figure 3. Values of the speed of sound and the resultant propagation velocity of sound in the direction of the microphone array were compiled and are presented in figure 4. Values of the ICAO atmosphere (ref. 8) are also shown in the figure. It is seen that the resultant propagation velocity of sound is generally linear with altitude and hence no atmospheric focusing of the sound field would be expected (ref. 9).

Lift-off of the Atlas 11-C vehicle was accomplished at 10:53 a.m. in clear weather; the surface temperature was 81° F. Rawinsonde measurements were not markedly different from those for the Atlas 10-D vehicle.

Vehicle Positioning and Trajectory

The positioning of the vehicle as a function of time was obtained for correlation with the noise measurements with the aid of phototheodolite equipment and high-speed cameras located in or near the launch complex and from equipment within the vehicle. Positioning data used in the presentation of the near-field data of this report are believed to be accurate within ±5 feet. Likewise, the far-field positioning data are believed to be accurate within ±50 feet.

RESULTS AND DISCUSSION

Noise measurements were taken during both captive firing and launch firing of the Atlas vehicles. Prior to lift-off the vehicle is essentially in the same nonmoving condition as during the captive firing. Therefore, for the presentation of these results the data are divided into two launch phases: the nonmoving or pre-lift-off phase and the moving or post-lift-off phase. Sound pressure levels in decibels (ref. 0.0002 dyne/cm^2) and spectra are presented for both the nonmoving and moving phases of launch.

Nonmoving Phase of Launch

During captive firings noise measurements were obtained along the longitudinal axis of one vehicle from the spacecraft to the region near the nozzle exit and at radial locations 180° around the launch vehicle at the instrument bay. Data were also obtained on the ground surface out to a distance of about 500 feet. For the second launch vehicle, noise measurements were obtained during the pre-lift-off phase of launch at a station about 3,500 feet from the vehicle. In figures 5 to 7 are presented overall sound pressure data and frequency spectra, and in figures 8 and 9 are presented the pressure time histories obtained during the nonmoving phase of launch.

Overall sound pressure levels and spectra.- Data obtained along the longitudinal surface of the vehicle are shown in figure 5. In this figure the sound pressure levels as a function of frequency in octave bands are shown for three locations along the length of the vehicle from the nozzle exit plane y. It is seen that the overall noise levels decrease from 154 db near the nozzle exit to 144 db at the Mercury spacecraft. In the lower frequency bands the noise level variation along the vehicle is limited to about 11 db, whereas in the higher frequency bands the variation approaches 20 db.

In figure 6 are shown the overall noise levels and spectra for three microphone positions located around the circumference of the launch vehicle in the vicinity of the instrument bays (y = approx. 35 feet). Noise levels measured along the side of the vehicle nearest to the deflected exhaust ($\alpha = 0^{\circ}$ in fig. 6) were about 5 db greater than measured values at $\alpha = 90^{\circ}$ and about 6 db greater than measured values at $\alpha = 180^{\circ}$. These results suggest the possibility that some acoustic shielding is provided by the vehicle.

In figure 7 are shown overall sound pressure levels and spectra at five locations radially outward from the launch vehicle (x = 5 to 3,500 feet). Data for four locations were obtained along the ground surface in a direction opposite ($\alpha = 180^{\circ}$) from the exhaust of the 10-D vehicle. Data at x = 3,500 feet were obtained from the 11-C vehicle at an azimuth angle of 45° from its exhaust. The noise levels are seen to decrease generally with distance from the launch vehicle, the greatest decrease being associated with the higher frequency bands. At x = 3,500 feet the spectrum is markedly different from the others shown, due probably to both the increased distance and the difference in azimuth angle.

Sound-pressure time histories.- A sound-pressure measurement was obtained for a location near the base of the service tower (x = 23 feet) during a captive firing and is illustrated in figure 8. The time history illustrated represents a 20-second-duration firing and contains data for ignition, rated thrust, and burnout phases of engine operation. During ignition and burnout, peaks were noted to occur in the sound-pressure-level time-history curve. Time histories of the instantaneous sound pressure during each of these phases of the engine operation were also obtained. Samples of the data records which are high-speed, cathode-ray oscilloscope photographs are presented in figure 9. The amplitude scales of all three pressure time histories are directly comparable.

Relatively high sound pressure amplitudes are noted during both the ignition and burnout phases of the engine operation, and the peak-to-peak amplitudes are

as much as five times as large as those which occur during rated thrust operation. It can also be seen that these high amplitudes are associated with much lower frequencies than the frequencies that occur during the time of rated thrust operation of the engine. The presence of the low-frequency noise is not fully understood but may result from combustion instabilities, nozzle-flow instabilities, or combustion-chamber resonances.

Noise-pressure amplitude distributions.- Because of the obvious importance of the response of structures to noise, a study has been made of the amplitude distributions of the instantaneous noise pressure. The noise time histories were played back into an electronic counting device which was adjusted to count the number of times the instantaneous pressure signal exceeded, or crossed, a predetermined reference value. This procedure was repeated for several reference values so that an amplitude distribution could be obtained. The instrument was adjusted to respond to crossings associated with increasing positive or increasing negative values of pressure and did not respond to crossings associated with decreasing positive or negative values of instantaneous pressure. For purposes of presentation in figure 10, the number of crossings above each selected reference level are normalized to those associated with the lowest reference level and are shown as a function of σ, which is defined as the ratio of the reference pressure to the true root-mean-square pressure.

Sound-pressure data are presented for a near-field location (23 feet) and a far-field location (516 feet) based on a 10-second experimental sample and are compared with a theoretical normal (Gaussian) distribution curve. The data obtained at the far-field measuring station seem to follow the theoretical-distribution curve very well. At the near-field measuring station, however, it can be seen that the data do not follow the theoretical-distribution curve. In particular, the large-amplitude peaks are fewer in number than the theory predicts. This may be due to possible distortion of the intense sound waves during propagation in the atmosphere in the near field.

Moving Phase of Launch

The overall sound pressure levels measured at several microphone locations for the launch condition are shown in figure 11 as a function of time. Data are presented for values of x from 23 feet to 516 feet, as indicated in figure 2, for the Atlas 10-D vehicle. An additional curve for $x = 3,500$ feet was obtained for the Atlas 11-C vehicle which also had a vertical trajectory. The data shown after lift-off apply to the phase of flight during which the vehicle is accelerating and, hence, both the distances and directions of the vehicles relative to the microphones are changing as a function of time. It can be seen that a peak in the sound-pressure-level time-history curve occurs for each microphone station, the higher sound pressure levels being associated with the closer stations (170 db at $x = 23$ feet and 116 db at $x = 3,500$ feet). The peak value of sound pressure level and its time of occurrence is believed to be dependent upon the elevation angle $(90^\circ - \beta)$ as well as the distance of the microphone station relative to the vehicle.

The time intervals for which various values of sound pressure level are exceeded have been determined from data of the type shown in figure 11 for four

of the microphone locations; these results are shown in figure 12. Straight lines have been faired arbitrarily through the data points obtained at each location to indicate trends. It can be seen that the large time intervals are, for each station, associated with the lower sound pressure levels. It can also be seen that the time intervals for which a given sound pressure level is exceeded are generally longer for the measuring stations closer to the vehicle. This second result applies particularly for the higher sound-pressure-level values associated with the initial part of the vehicle flight trajectory. The higher rates of change of sound pressure level with time seem to be associated with the closer measuring stations so that, when the vehicle is at a great distance from the launch site, essentially the same noise exposures occur at all of the measuring stations.

The maximum sound pressure levels measured at each station during launch are plotted at the corresponding horizontal distances from the launch site in figure 13. Also shown for comparison is a dashed line corresponding to the inverse distance relationship (6-db decrease per doubling of distance) normalized to data at $x = 100$ feet. The data, of course, apply for different times during the flight and, hence, also for different vertical positions of the vehicle. For a nearly vertical launch such as for these data, it can be seen that the inverse distance relationship fairly well predicts the change of maximum sound pressure level with distance, as would be expected.

The octave-band noise spectrum at each microphone location of figure 11 is given in figure 14 for the time of maximum overall sound pressure level. In general, it can be seen that the spectra obtained at the shorter distances contained relatively more high-frequency noise than those at the greater distances. This result is believed to be due mainly to the greater atmospheric losses at the higher frequencies during propagation since the orientation of the vehicle with reference to the measuring stations was essentially the same at the time for which these spectra apply.

From the overall-sound-pressure-level and octave-band-spectra time histories obtained for each microphone station and from the vehicle-position—time data, sound pressure level as a function of vertical distance of the vehicle during lift-off was determined. Sound pressure levels in various frequency bands are presented as a function of altitude of the vehicle in figure 15 for four horizontal locations. Both horizontal distance and altitude are expressed in terms of equivalent nozzle exit diameter. (Equivalent nozzle exit diameter is defined herein as the diameter of a nozzle having an exit area equivalent to the areas of the three rocket nozzles of the vehicle.) Each curve is seen to have a rather broad peak. At locations farther from the launch site in the horizontal direction, the maximum levels for a given frequency are associated with a higher vehicle altitude. For a given horizontal distance, the maximum value of sound pressure level for a high-frequency band is noted to occur at a lower altitude of the vehicle than does the maximum sound pressure level for a low-frequency band. This result is a confirmation of the characteristic radiation patterns of rocket engines as determined from several other studies (refs. 1 to 6) in that the lower frequencies are radiated generally in the direction of the jet axis, whereas the higher frequencies are radiated generally normal to the axis.

Comparison With Scout-Vehicle Launch Noise Measurements

To provide information useful for future estimation of launch-site noise levels, the present data are compared with similar data for a Scout vehicle which had a solid-propellant rocket engine with a low thrust and a higher initial acceleration. The noise data have been adjusted by means of the inverse distance law to a slant distance of 1,000 feet. These adjusted values, with the maximum value from the Atlas 10-D vehicle as a reference, are plotted in figure 16 as a function of azimuth angle β, measured from the thrust axis at the rear of the launch vehicle to the measuring stations. Also plotted in the figure are data obtained under similar test conditions from the launch of a Scout vehicle at the NASA Wallops Station. The Scout vehicle had a solid-propellant rocket engine of about 100,000 pounds rated thrust, a launch angle of 78°, and an initial acceleration of about 1.8g. For purposes of comparison, the Scout data have been adjusted to higher values by 5.6 db in order to account for the difference in engine thrust. It can be seen that the two sets of data are in agreement within about 4 db over a wide range of azimuth angles. These differences may be accounted for, at least in part, by the changes in the sizes and velocities of the vehicles and in the atmospheric and terrain conditions at the two launch sites. Of note are two Scout data points (observed at one station) which lie well above the Atlas data. This deviation is believed to be due to an inversion layer in the atmosphere which caused a momentary increase in the noise levels, a factor that must be considered in predicting noise at large distances particularly when the ray paths are nearly parallel to the ground.

CONCLUSIONS

Near-field and far-field noise measurements during the captive firing and launch firing of a large rocket-powered vehicle indicate the following conclusions:

1. The sound pressure levels along the exterior of the vehicle vary from about 154 db near the nozzle exit to about 144 db in the region of the payload when a turning bucket is in use. The sound field for this condition is not symmetrical about the vehicle, the sound-pressure-level value being about 6 db lower on the side of the vehicle opposite the exhaust jet.

2. For short periods of time during ignition and burnout, the measured sound pressures in the near field were about five times as large as those measured for the rated thrust condition.

3. The amplitude distribution of the far-field sound-pressure time history followed the theoretically predicted values of a Gaussian distribution. In the near field, however, there were fewer large amplitude peaks than were predicted by theory.

4. During launch, sound-pressure-level values as high as 170 db were measured at a horizontal distance of 23 feet and as high as 116 db at a distance of 3,500 feet.

5. Sound pressure levels above a given value persist longer at measuring stations close to the launch pad than at those at greater distances.

6. Radiation patterns observed during these launchings are not markedly different from those previously measured for static conditions and agree within about 4 db with Scout vehicle data adjusted to similar operating conditions.

Langley Research Center,
National Aeronautics and Space Administration,
Langley Station, Hampton, Va., August 14, 1962.

REFERENCES

1. Cole, J. N., Von Gierke, H. E., et al.: Noise Radiation From Fourteen Types of Rockets in the 1,000 to 130,000 Pounds Thrust Range. WADC Tech. Rep. 57-354, AD 130794, U.S. Air Force, Dec. 1957.

2. Mayes, William H., Lanford, Wade E., and Hubbard, Harvey H.: Near-Field and Far-Field Noise Surveys of Solid-Fuel Rocket Engines for a Range of Nozzle Exit Pressures. NASA TN D-21, 1959.

3. Mayes, William H., Edge, Philip M., Jr., and O'Brien, James S., Jr.: Near-Field and Far-Field Noise Measurements for a Blowdown-Wind-Tunnel Supersonic Exhaust Jet Having About 475,000 Pounds of Thrust. NASA TN D-517, 1961.

4. Anon.: The Noise Field of Jupiter Missiles. Rep. No. 659 (ABMA Contract No. DA-19-020-ORD-4685), Bolt Beranek and Newman, Inc., Dec. 28, 1959.

5. Anon.: Exterior Sound and Vibration Fields of a Saturn Vehicle During Static Firing and During Launching – Final Report. Rep. No. 764 (Contract No. DA-19-020-ORD-5038), Bolt Beranek and Newman, Inc., Aug. 29, 1960.

6. Dorland, Wade D.: Far-Field Noise Characteristics of Saturn Static Tests. NASA TN D-611, 1961.

7. Coleman, D. J., Jr.: Results of NASA-LOD Sound Pressure Level Measurements During SA-2 Launch. MTP-LOD-62-9. NASA George C. Marshall Space Flight Center, 1962.

8. Minzner, R. A., Ripley, W. S., and Condron, T. P.: U.S. Extension to the ICAO Standard Atmosphere - Tables and Data to 300 Standard Geopotential Kilometers. Geophys. Res. Dir. and U.S. Weather Bureau, 1958.

9. Perkins, Beauregard, Jr., Lorrain, Paul H., and Townsend, William H.: Forecasting the Focus of Air Blasts Due to Meteorological Conditions in the Lower Atmosphere. Rep. No. 1118, Ballistic Res. Labs., Aberdeen Proving Ground, Oct. 1960.

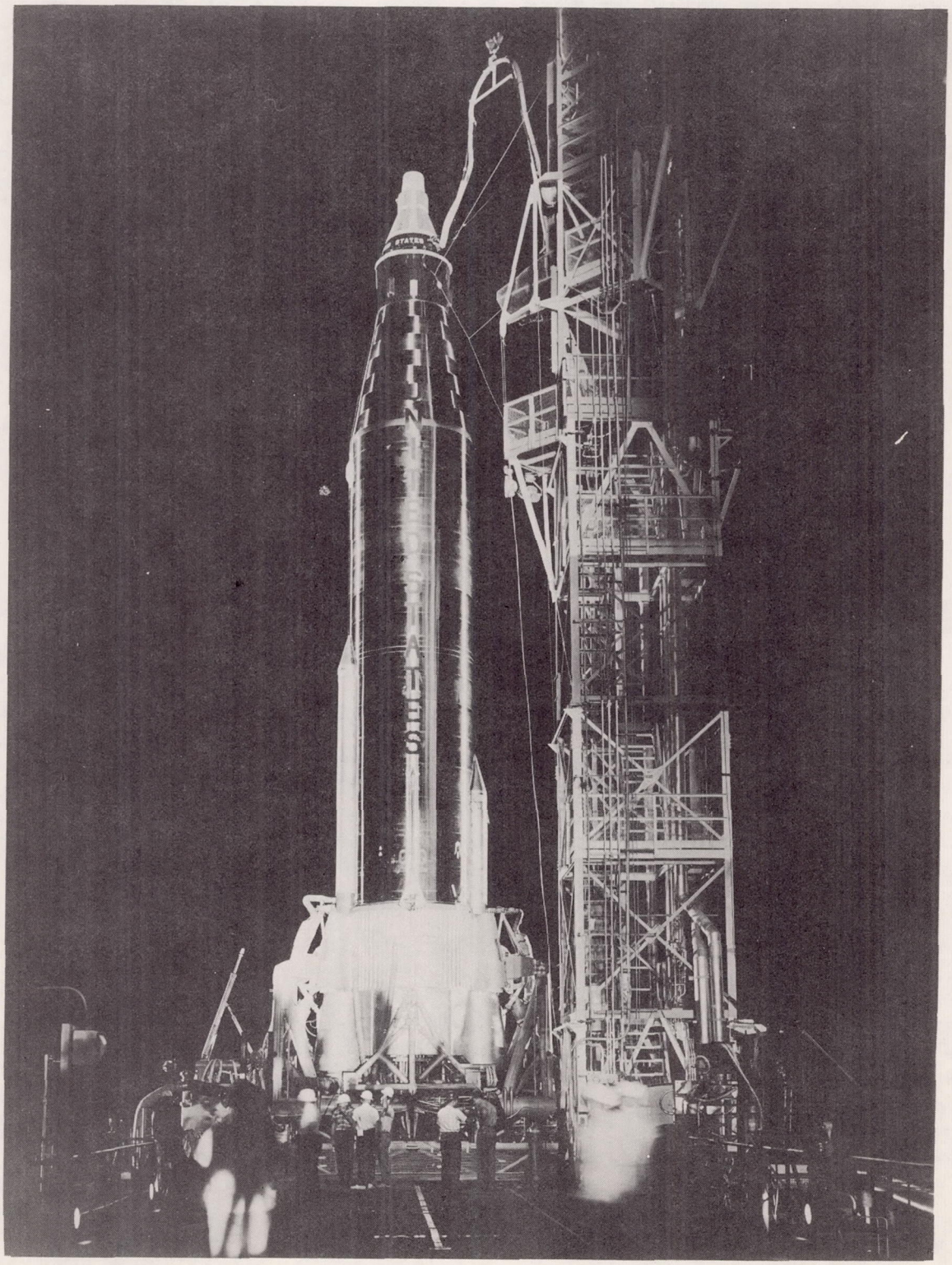

Figure 1.- Atlas 10-D test vehicle in launch position. S-61-2610

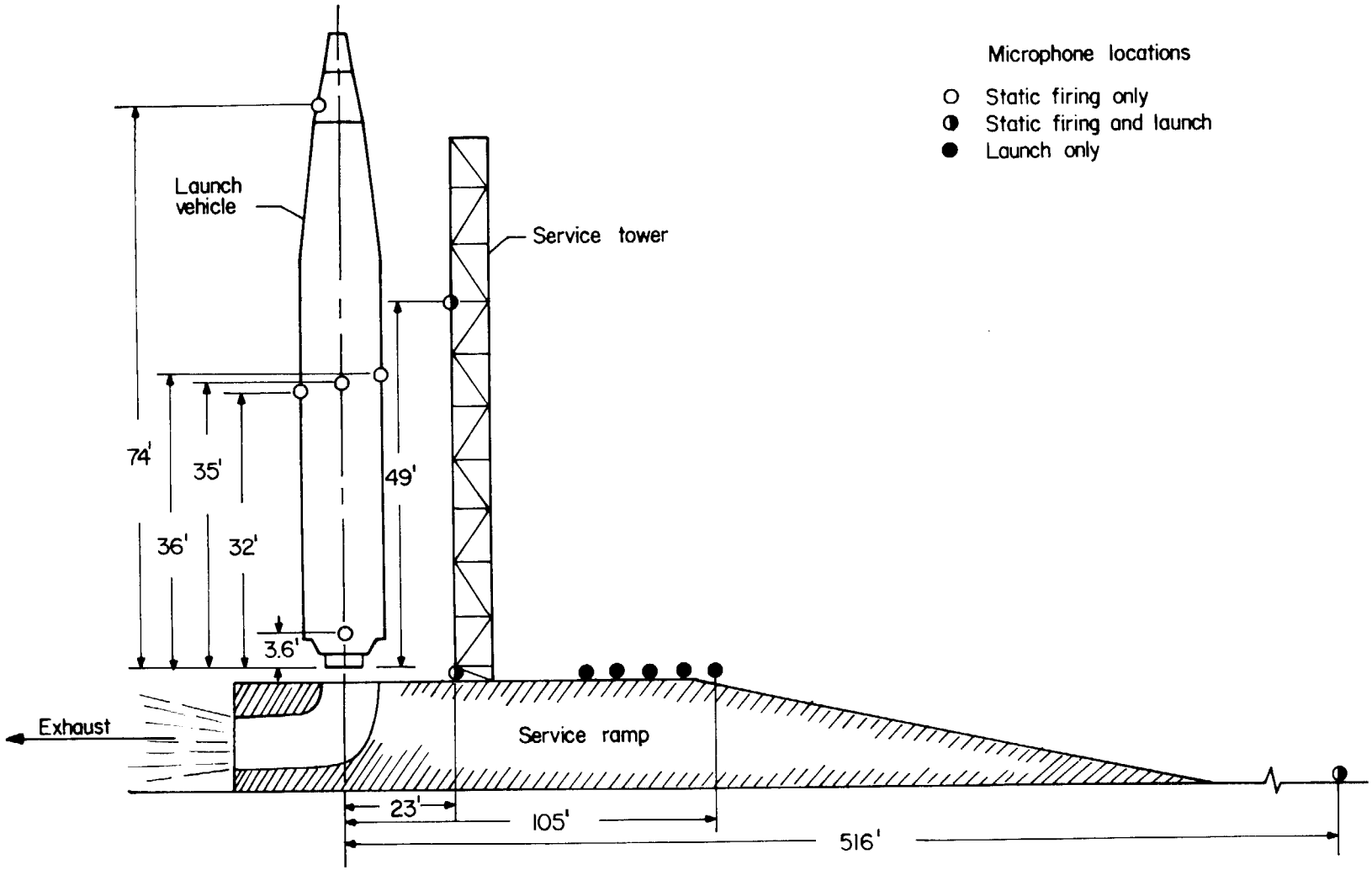

Figure 2.- Schematic diagram of Atlas 10-D launch vehicle and complex area showing microphone locations. (Direction of deflected exhaust is 15° east of north. Ground microphone array is located on side opposite the exhaust.)

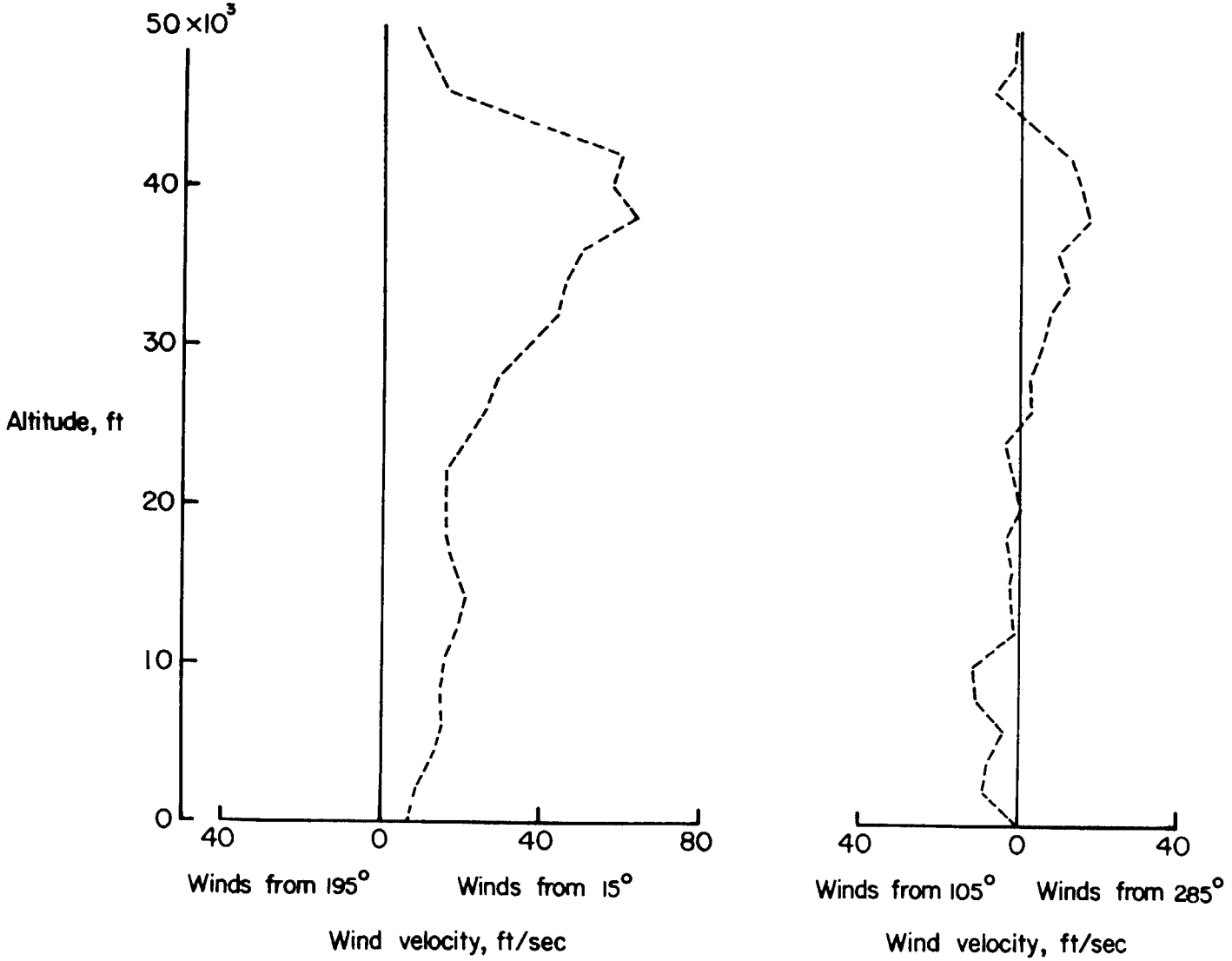

(a) Components along microphone array.

(b) Components perpendicular to microphone array.

Figure 3.- Wind-velocity components calculated from atmospheric soundings taken during the launching of the Atlas 10-D vehicle.

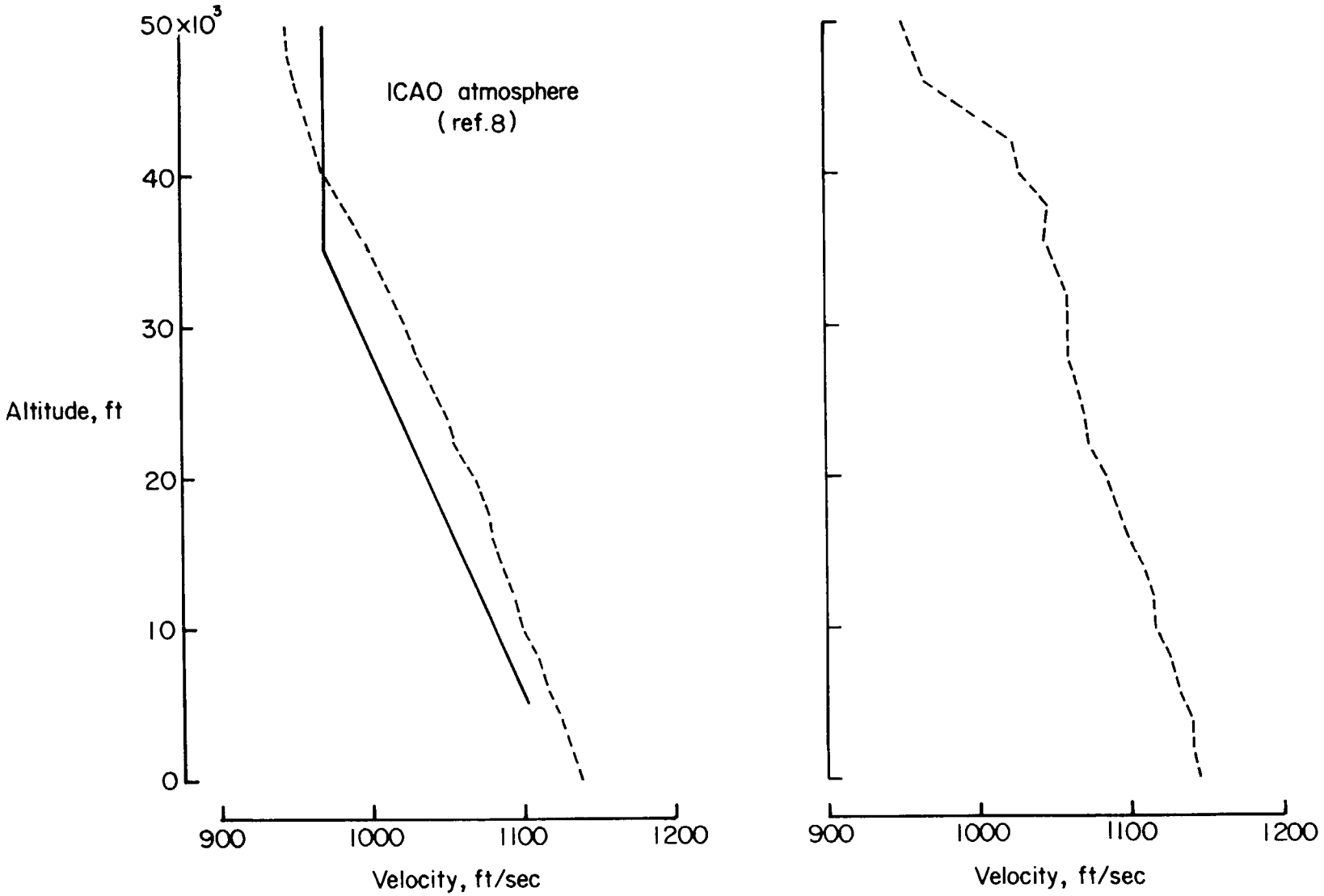

(a) Speed of sound.

(b) Resultant propagation velocity.

Figure 4.- Speed-of-sound and resultant-propagation-velocity values calculated from atmospheric soundings taken during the launching of the Atlas 10-D vehicle.

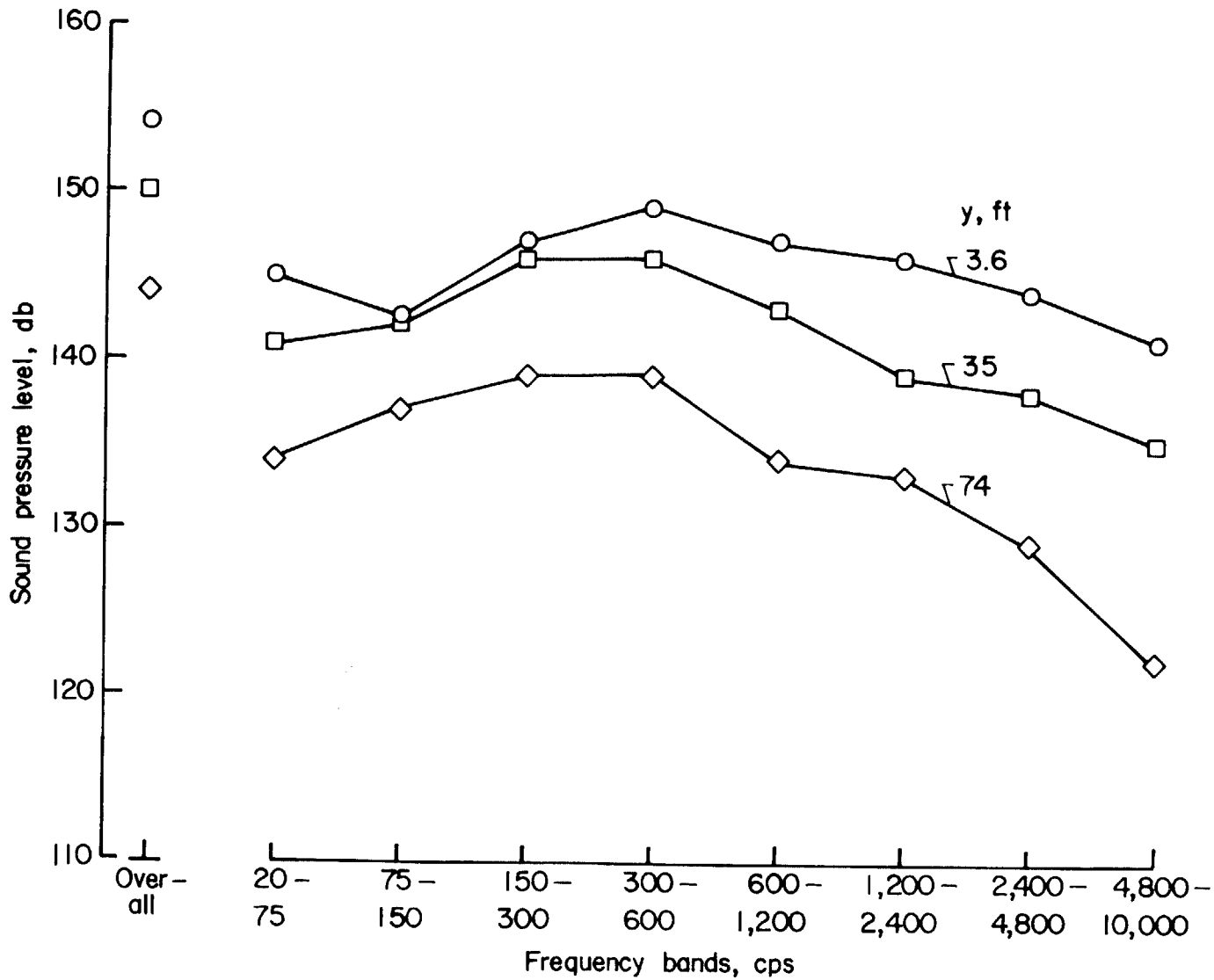

Figure 5.- Noise spectra at three stations along the longitudinal axis of the Atlas launch vehicle. (Nonmoving phase of launch.)

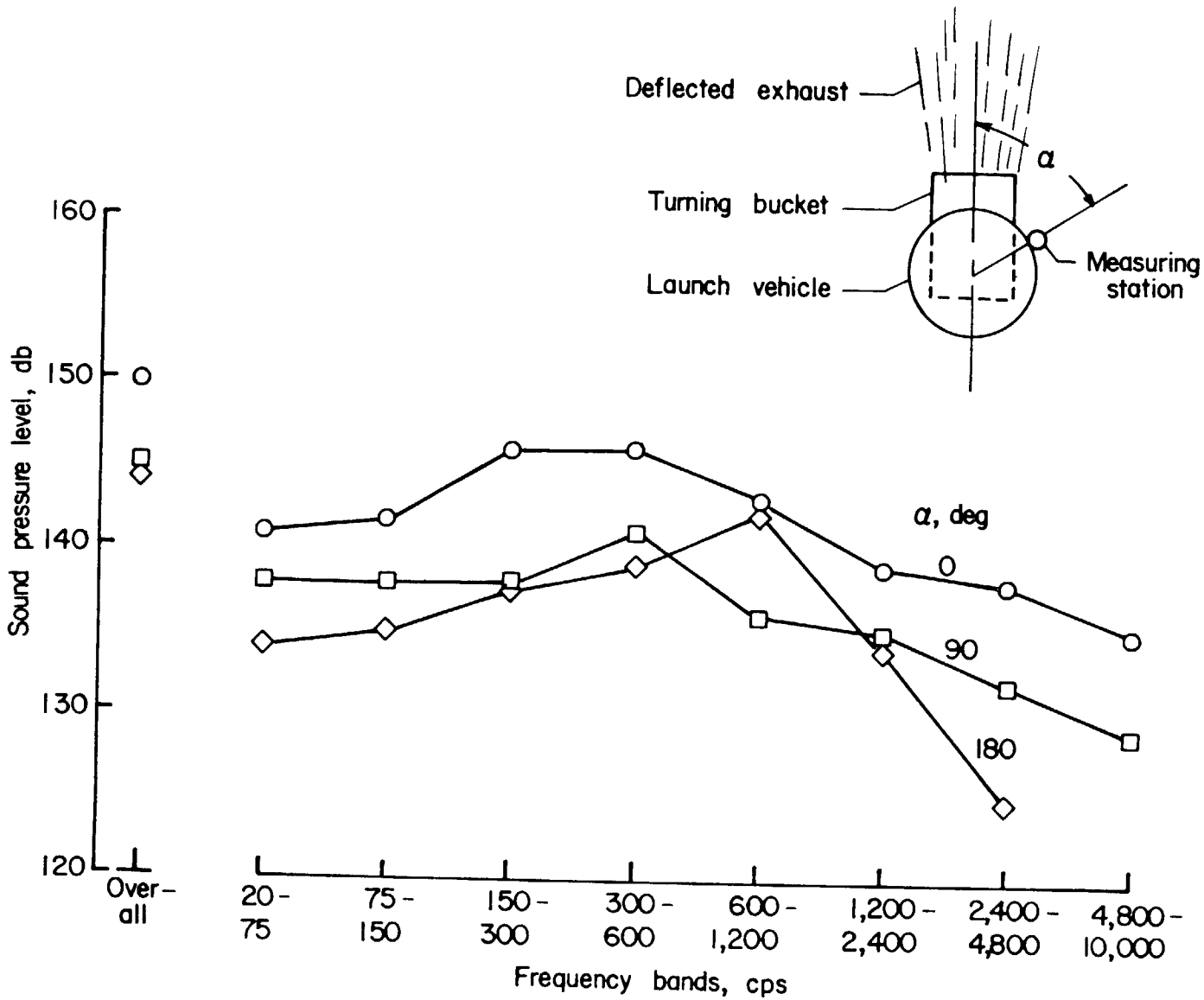

Figure 6.- Noise spectra at three circumferential stations on the Atlas launch vehicle in the vicinity of the instrument bay. (Nonmoving phase of launch.)

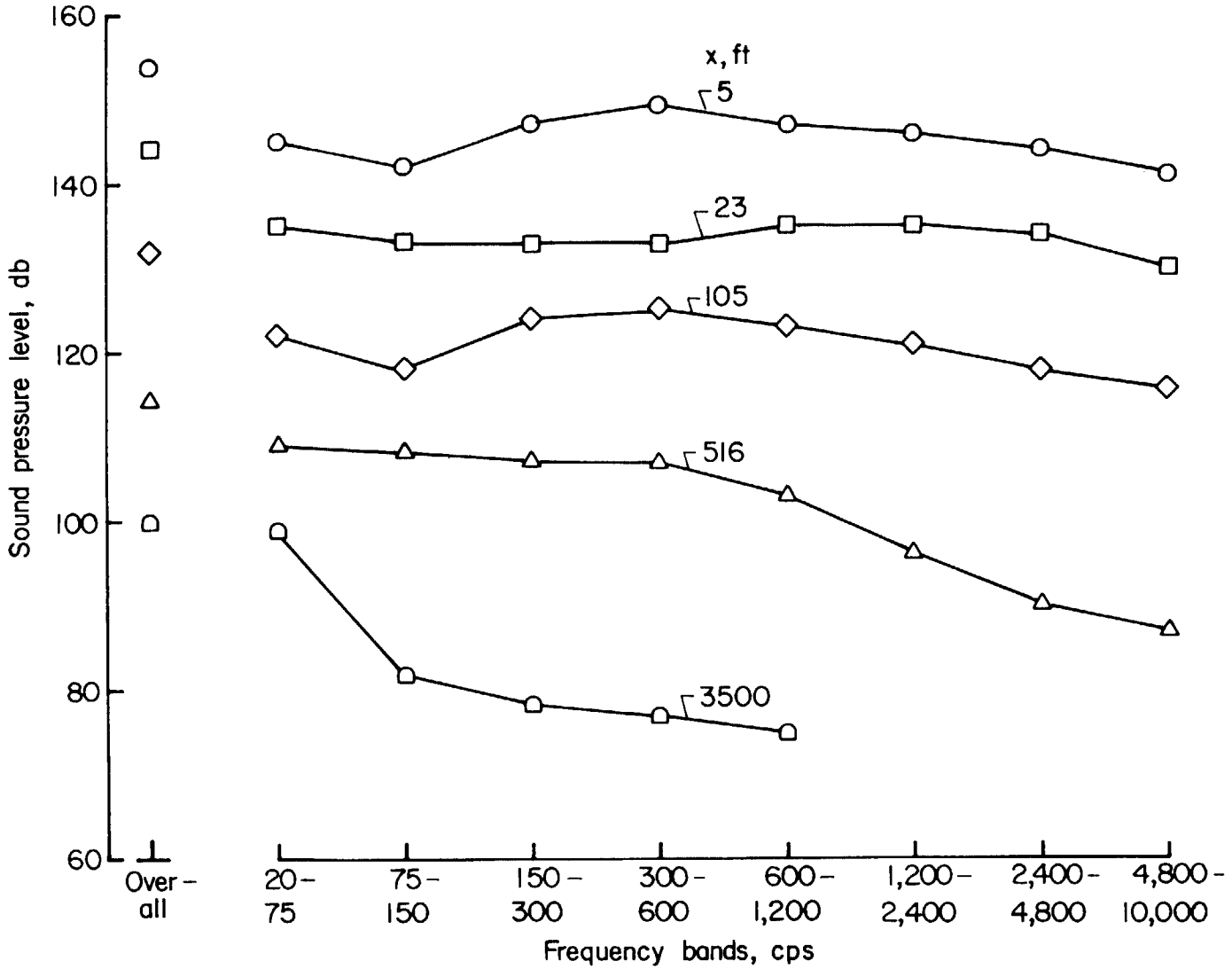

Figure 7.- Noise spectra at ground level for several measuring stations. (Nonmoving phase of launch.)

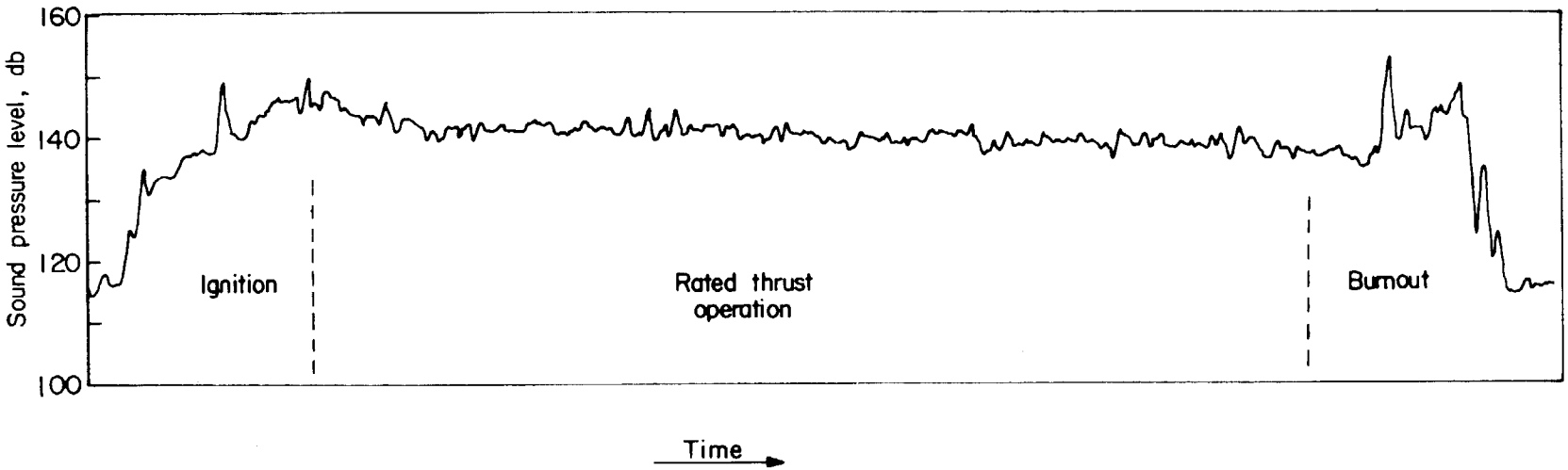

Figure 8.- Sound-pressure-level time history of Atlas 10-D captive firing at a station near the base of the service tower (x = 23 feet).

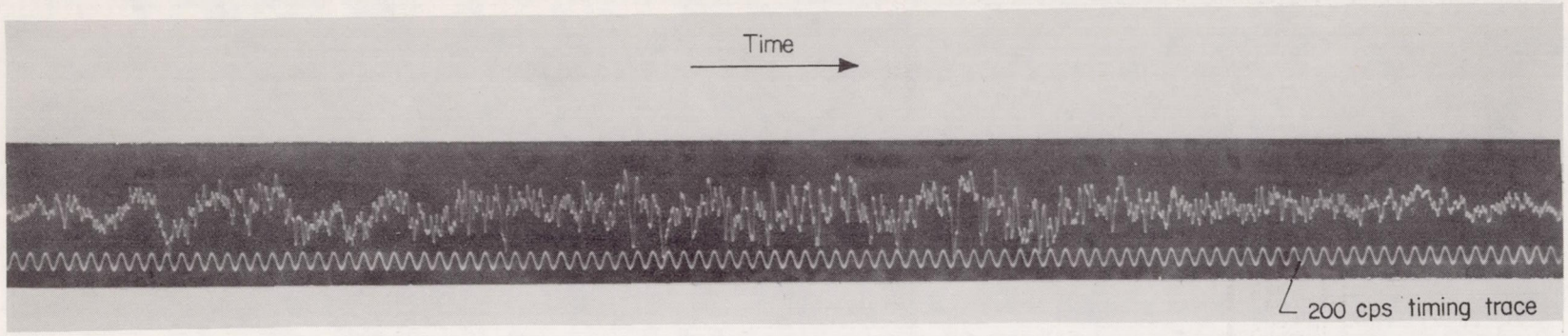

(a) Ignition.

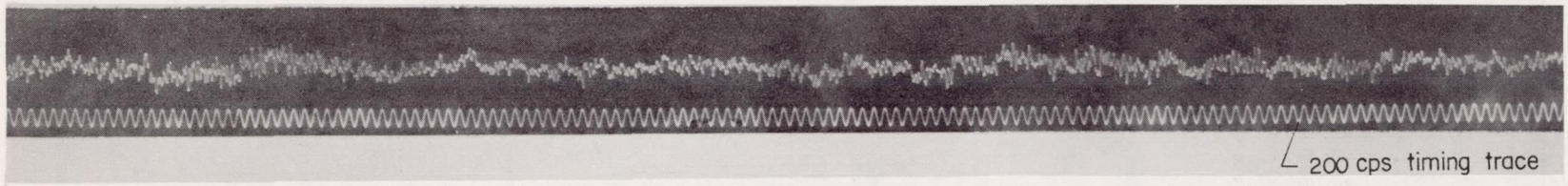

(b) Rated thrust operation.

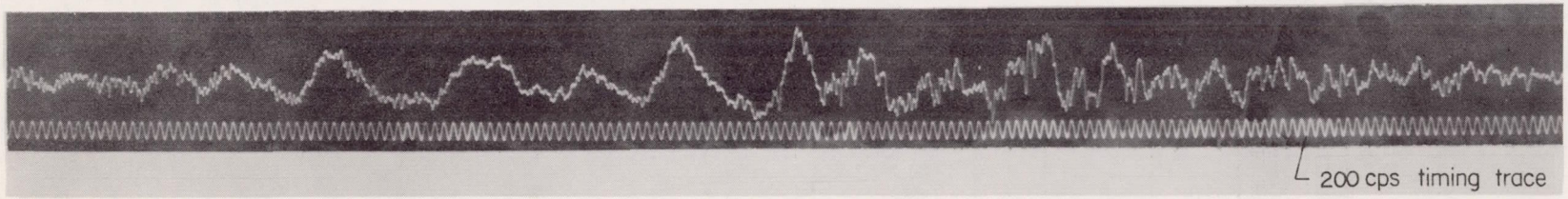

(c) Burnout.

Figure 9.- Instantaneous sound-pressure time histories for the Atlas 10-D captive firing. Sample data are shown for the ignition, rated thrust, and burnout phases indicated in figure 8.

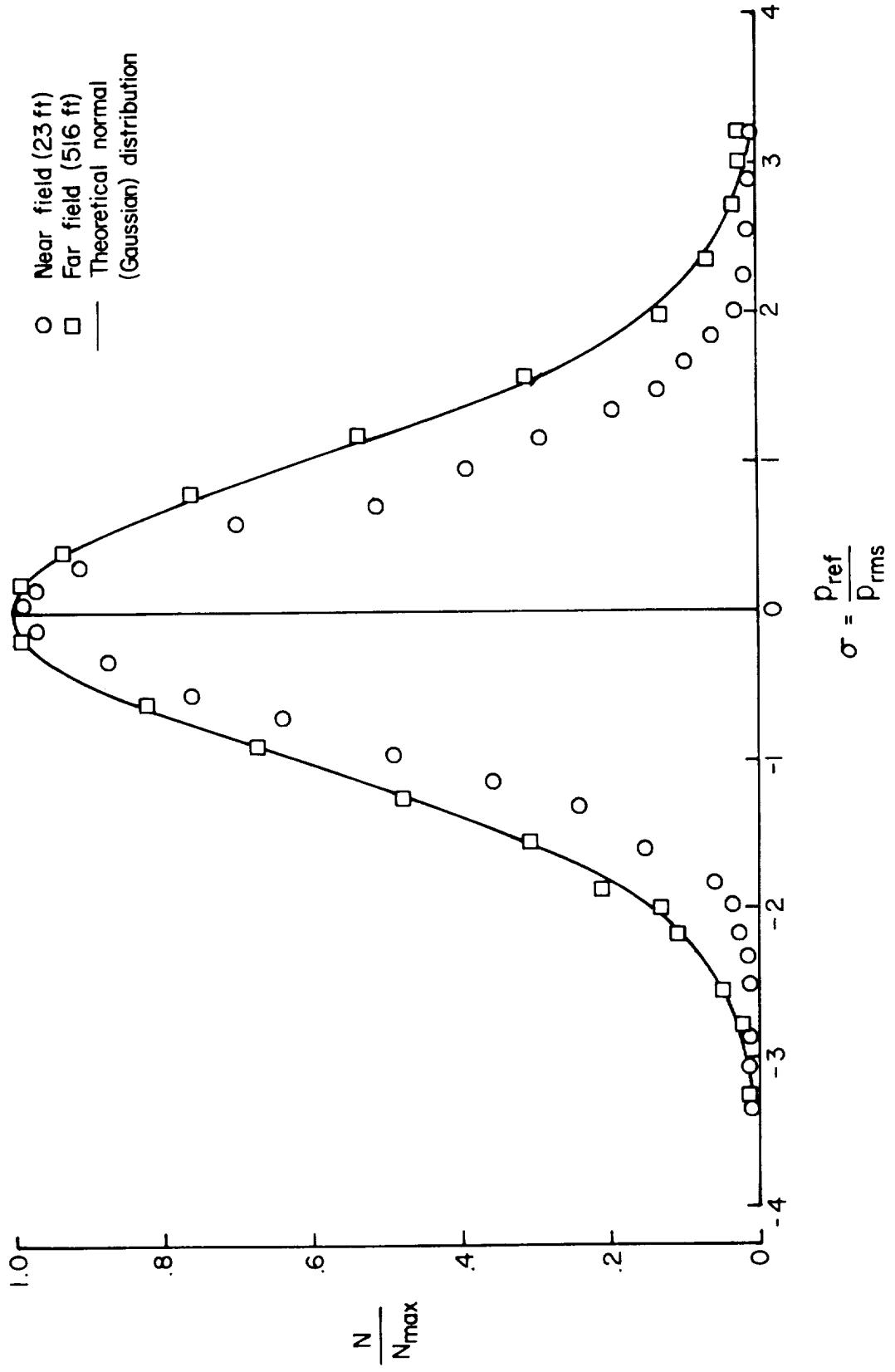

Figure 10.- Comparison of amplitude distributions of near-field and far-field sound pressures of the Atlas 10-D vehicle.

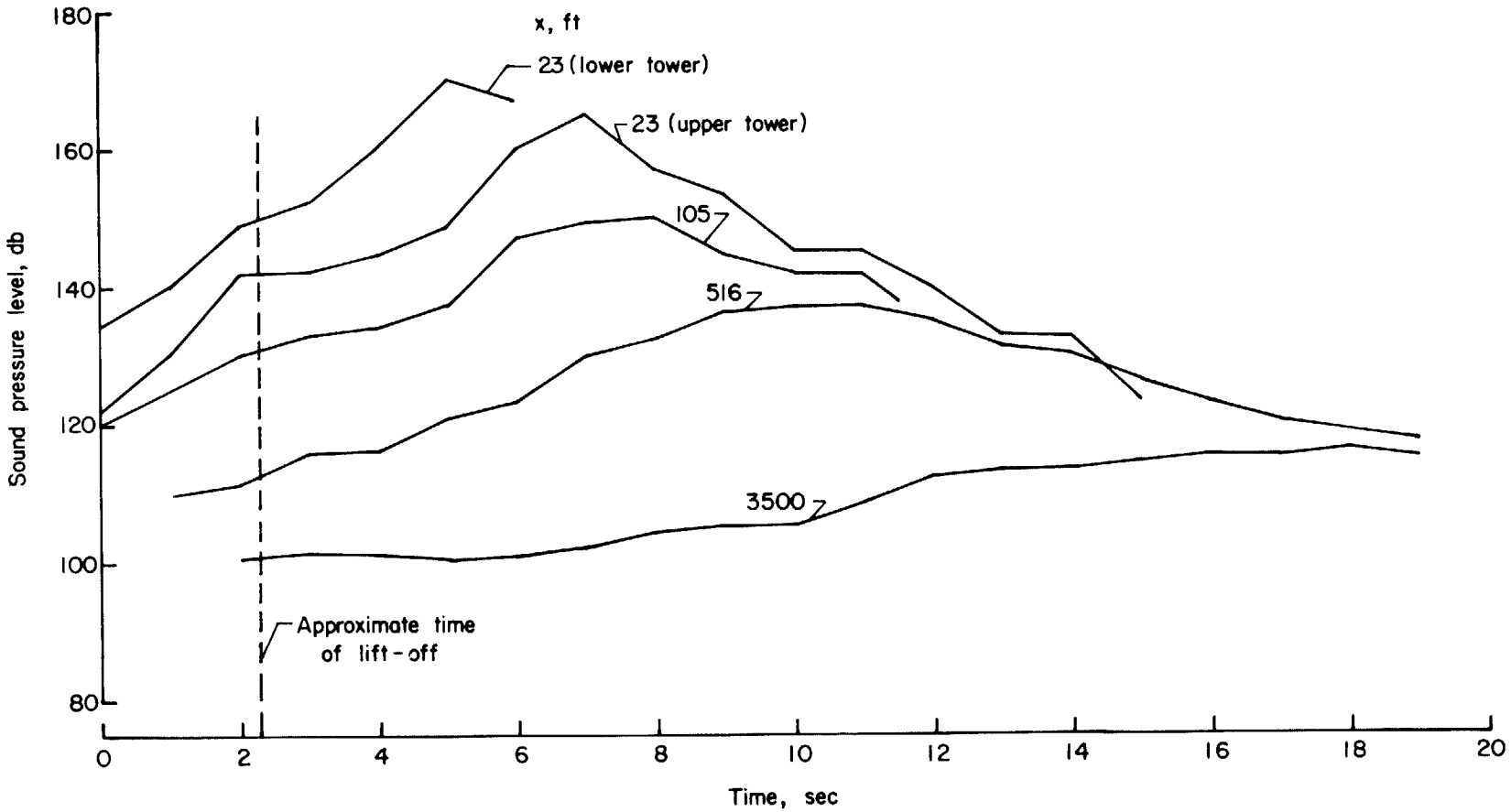

Figure 11.- Time history of overall sound pressure level at several measuring stations for the Atlas vehicles during launch.

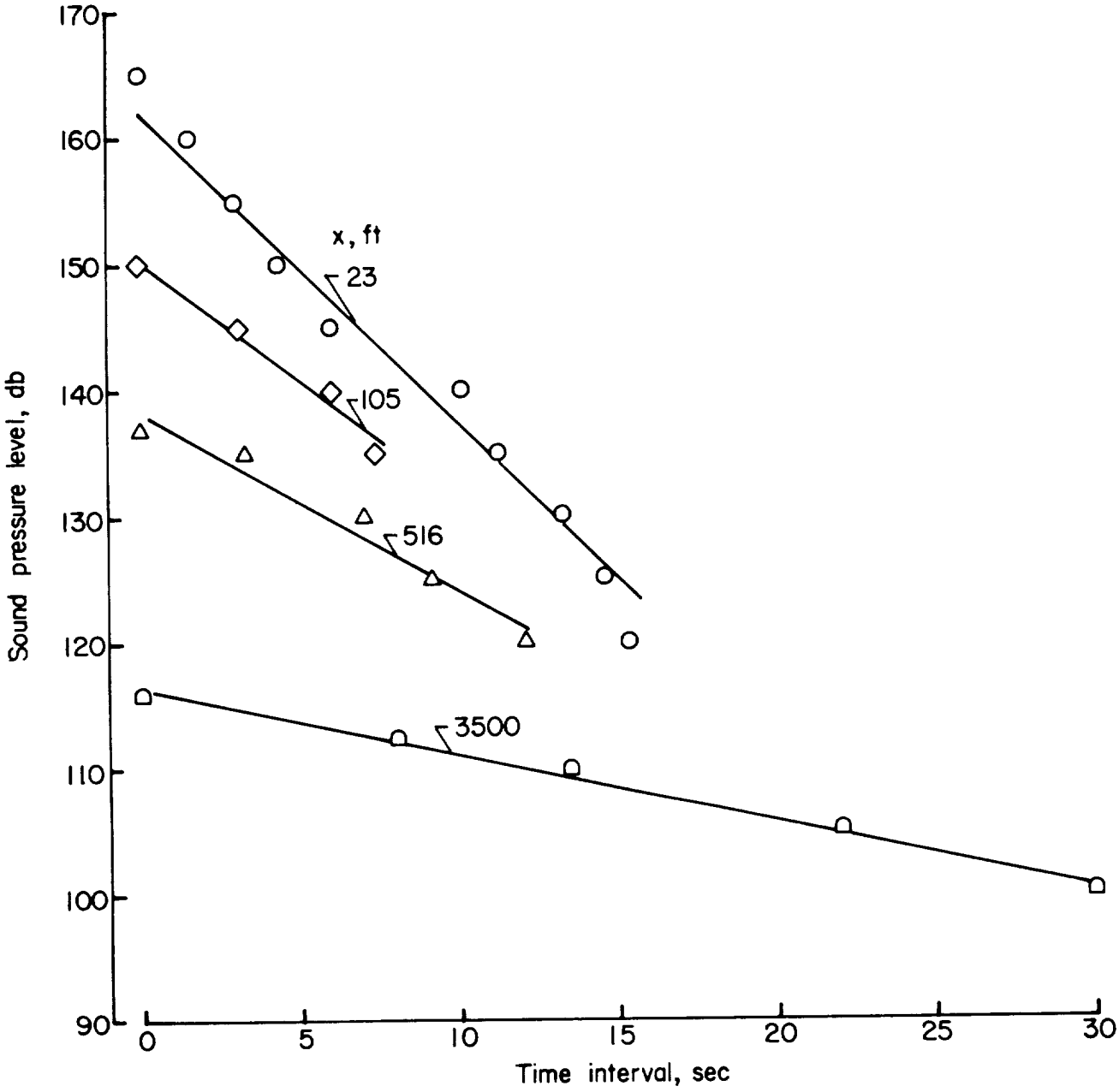

Figure 12.- Time interval in seconds for which the ambient overall sound pressure level exceeds given values at various distances from the vehicle during launch.

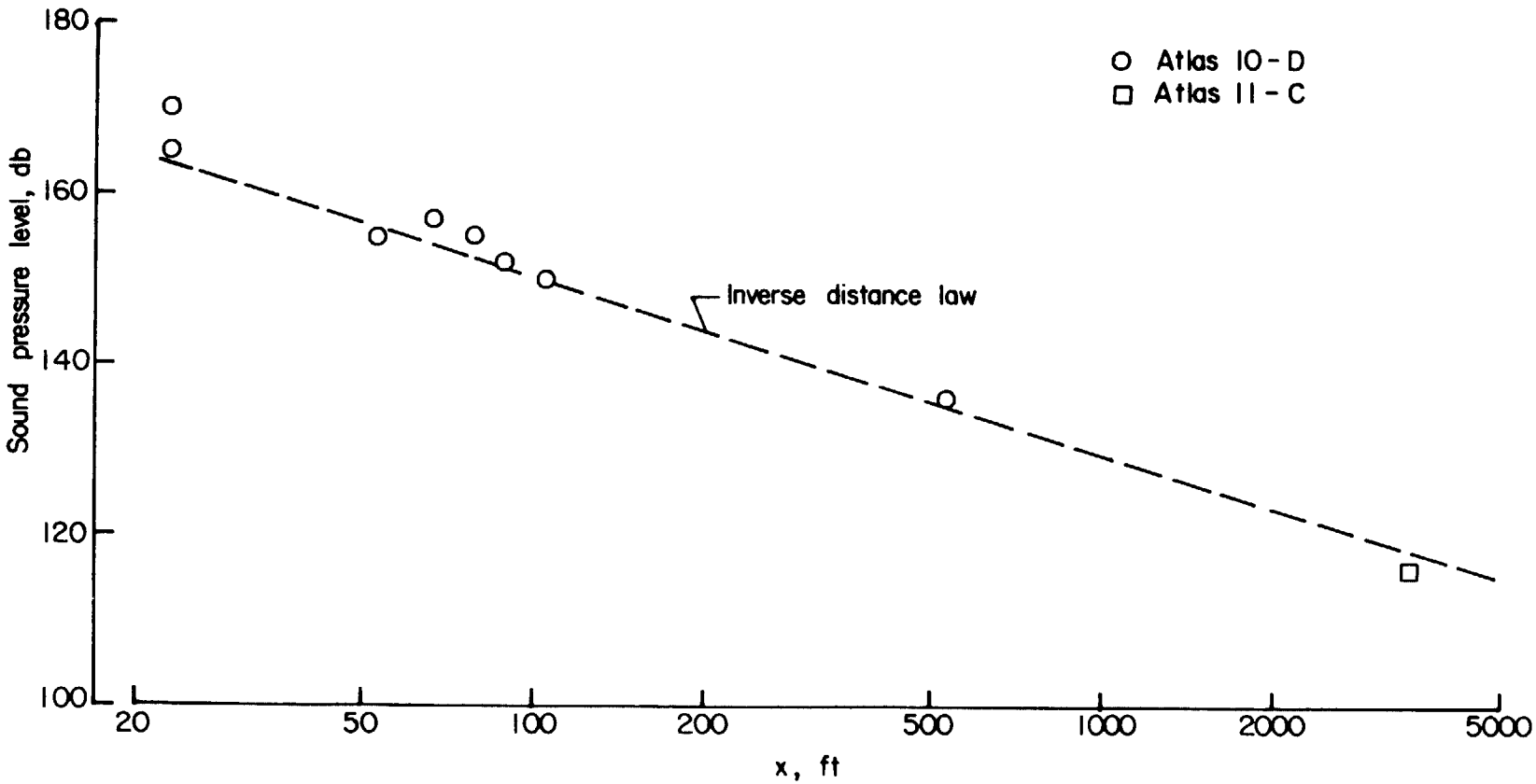

Figure 13.- Maximum sound pressure level as a function of horizontal distance from launch site in feet during vertical launching of two Atlas vehicles.

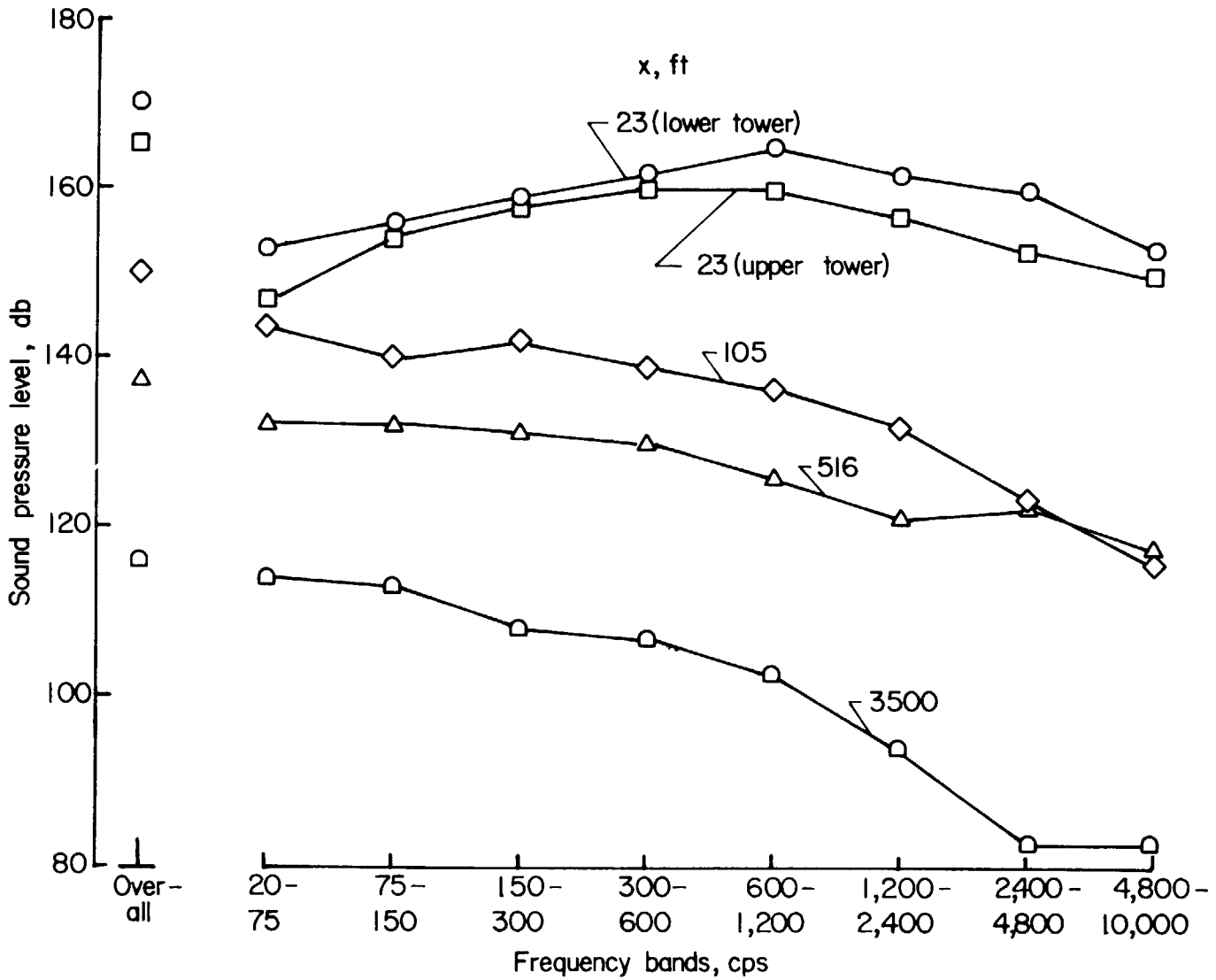

Figure 14.- Noise spectra at times of maximum sound pressure level at several stations for the Atlas vehicles during launch.

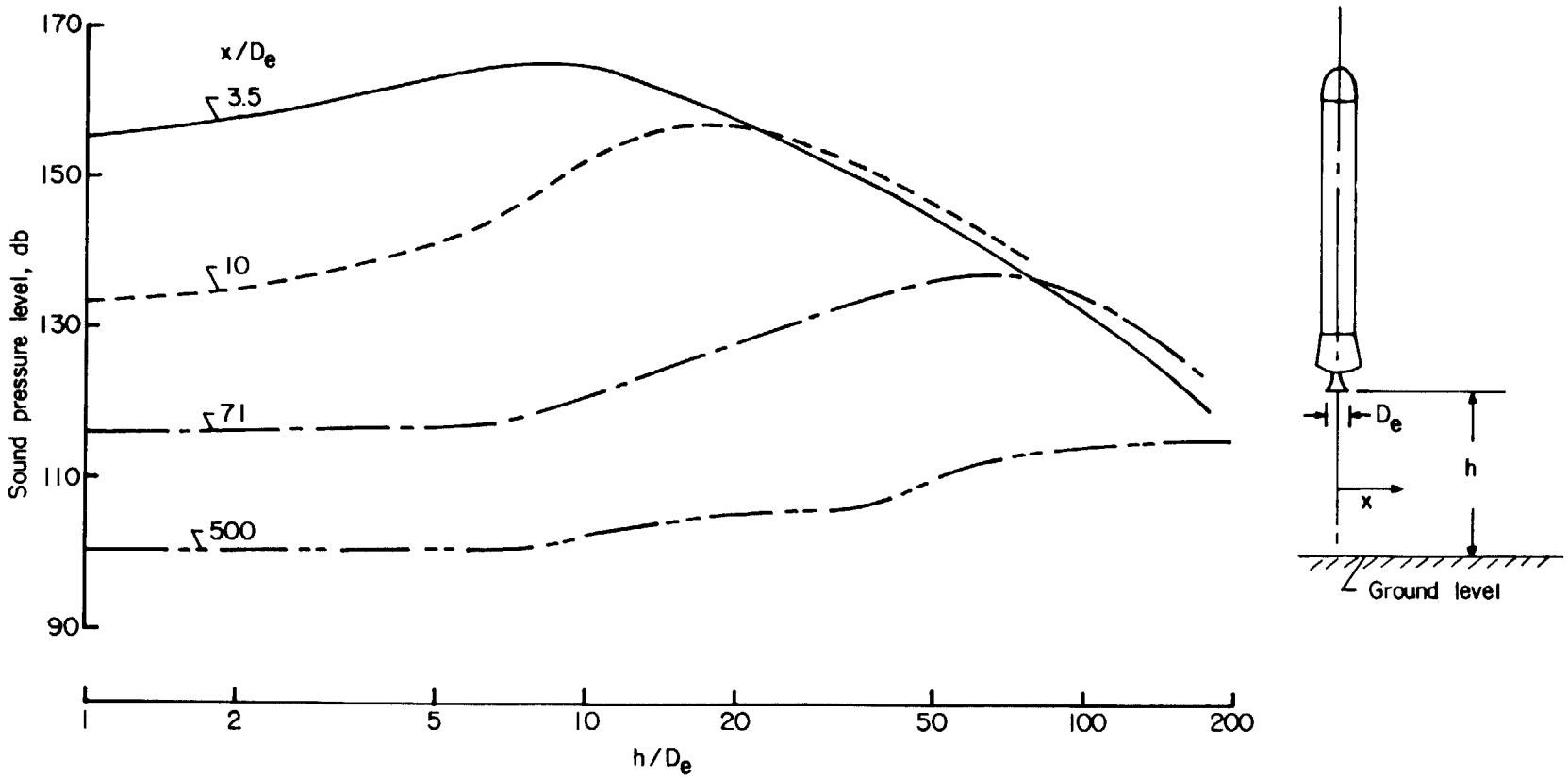

(a) 20 to 10,000 cps.

Figure 15.- Wide-band sound pressure levels at ground level as a function of vehicle altitude for four different measuring stations.

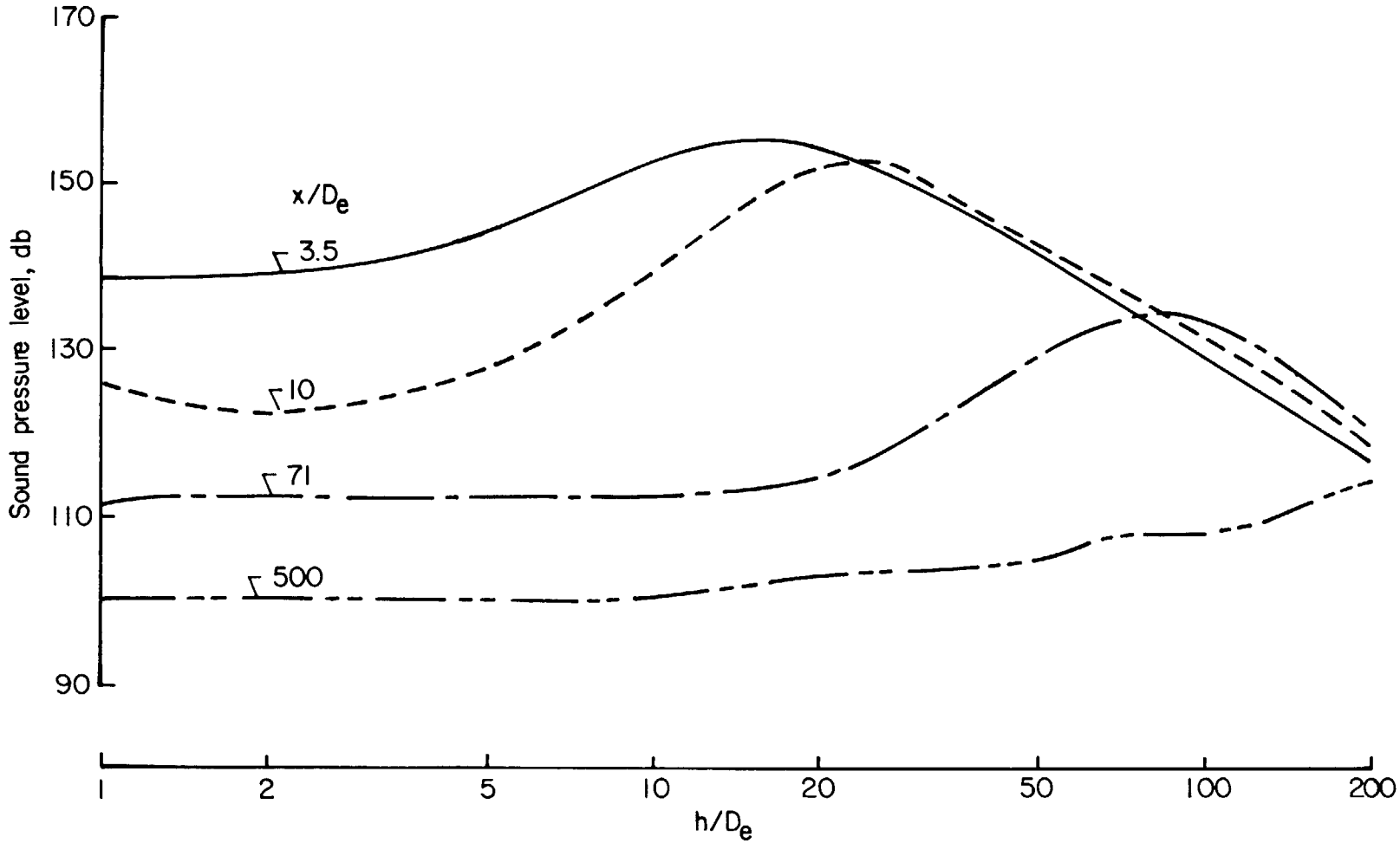

(b) 20 to 75 cps.

Figure 15.- Continued.

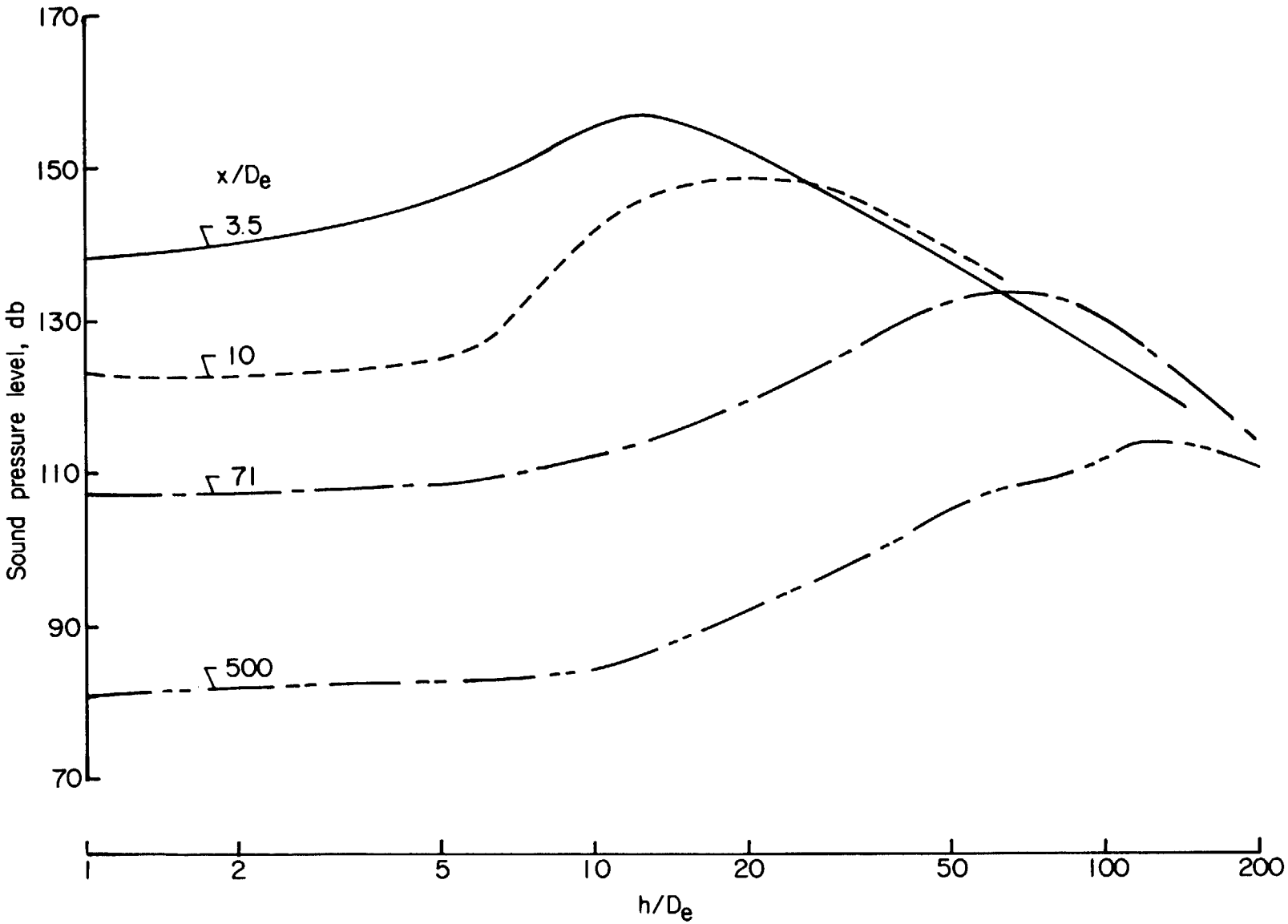

(c) 75 to 150 cps.

Figure 15.- Continued.

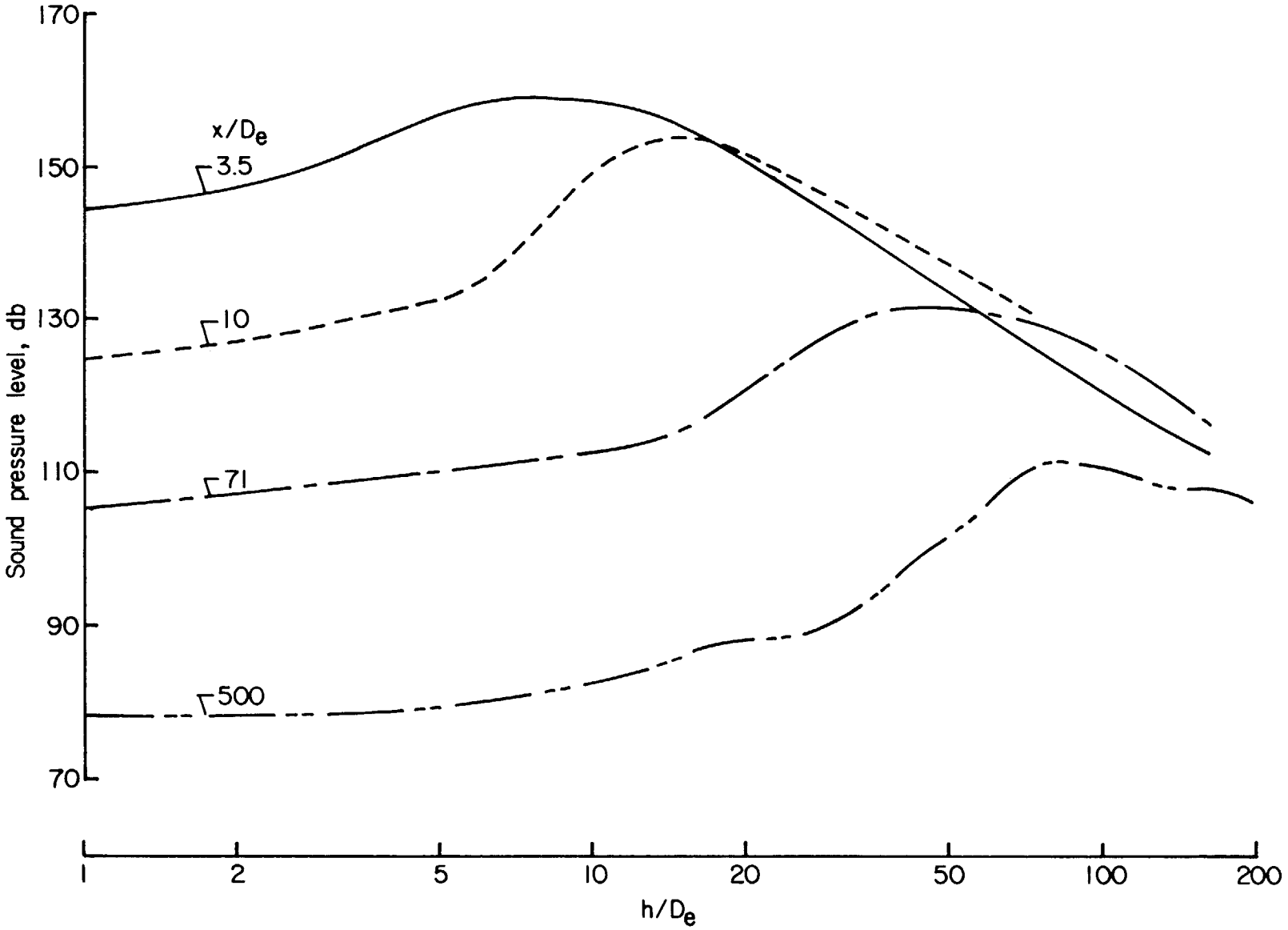

(d) 150 to 300 cps.

Figure 15.- Continued.

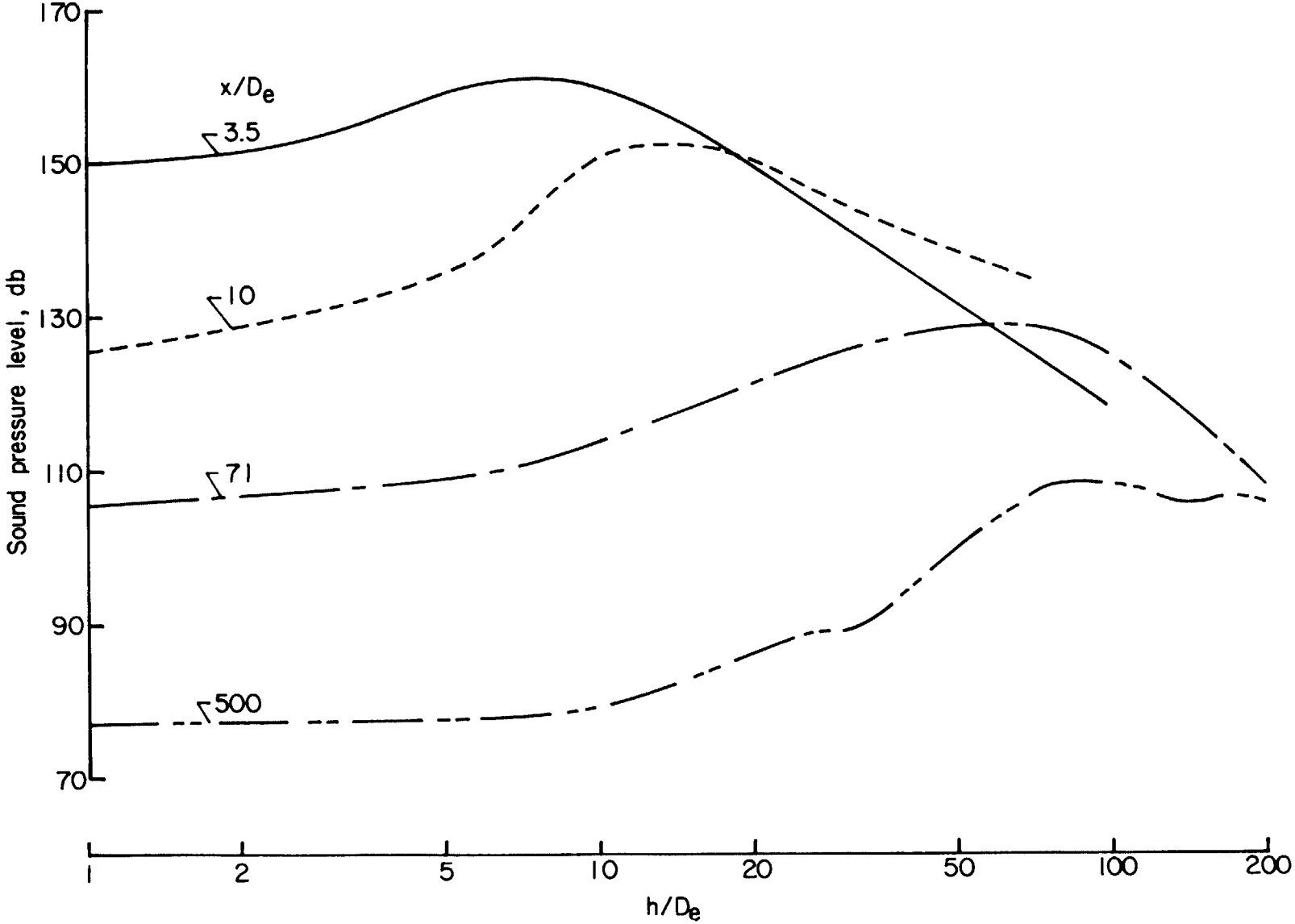

(e) 300 to 600 cps.

Figure 15.- Continued.

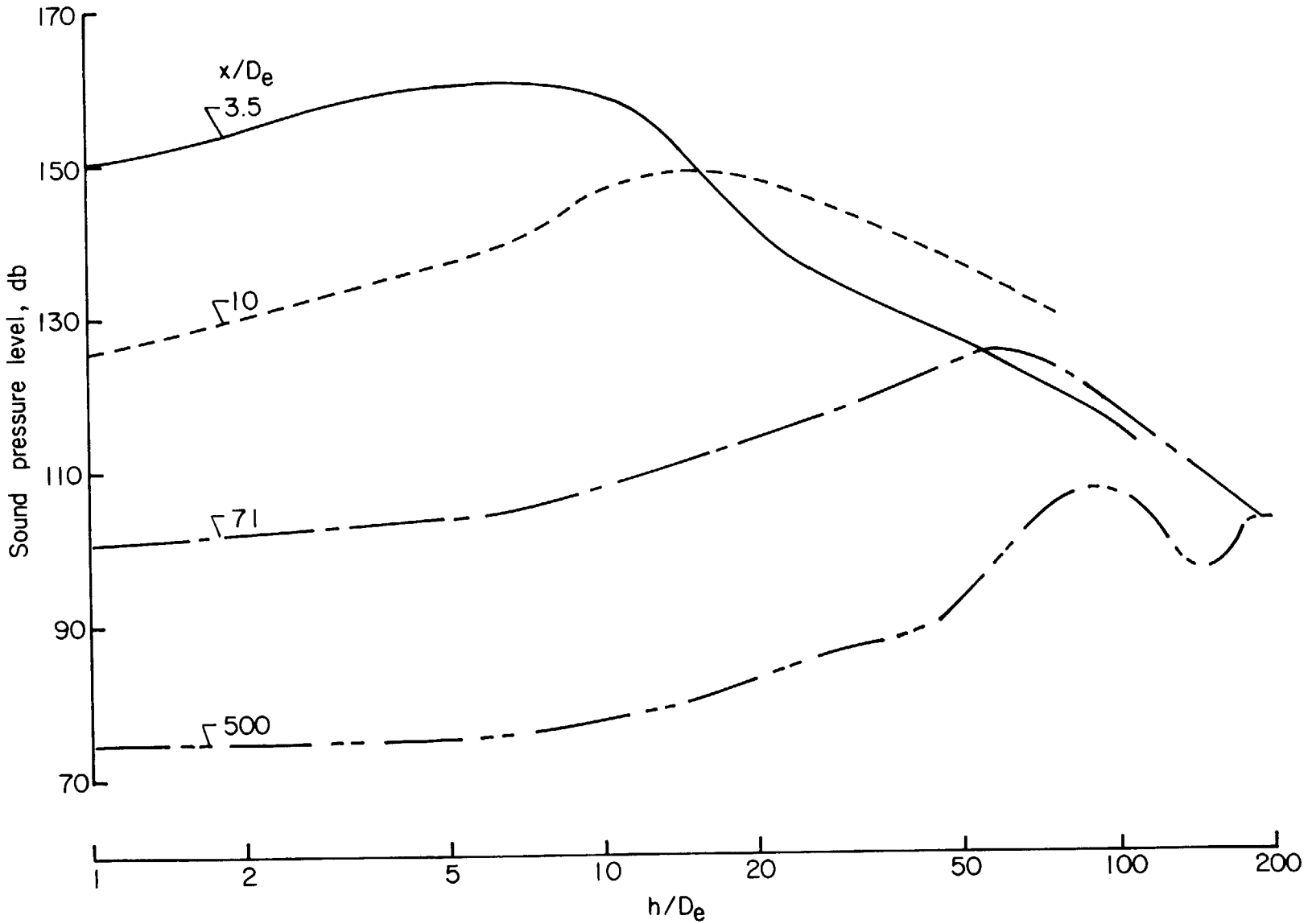

(f) 600 to 1,200 cps.

Figure 15.- Continued.

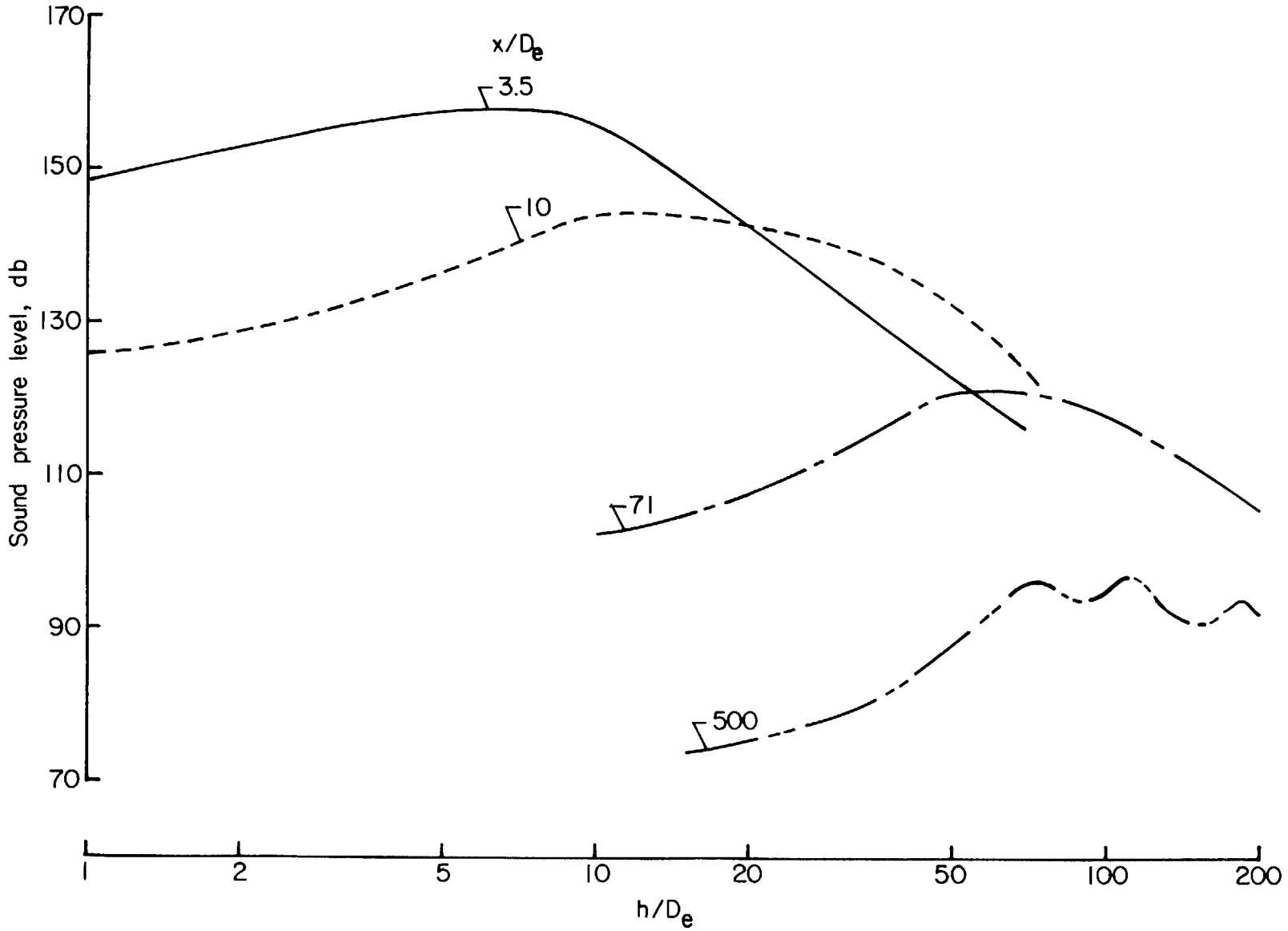

(g) 1,200 to 2,400 cps.

Figure 15.- Continued.

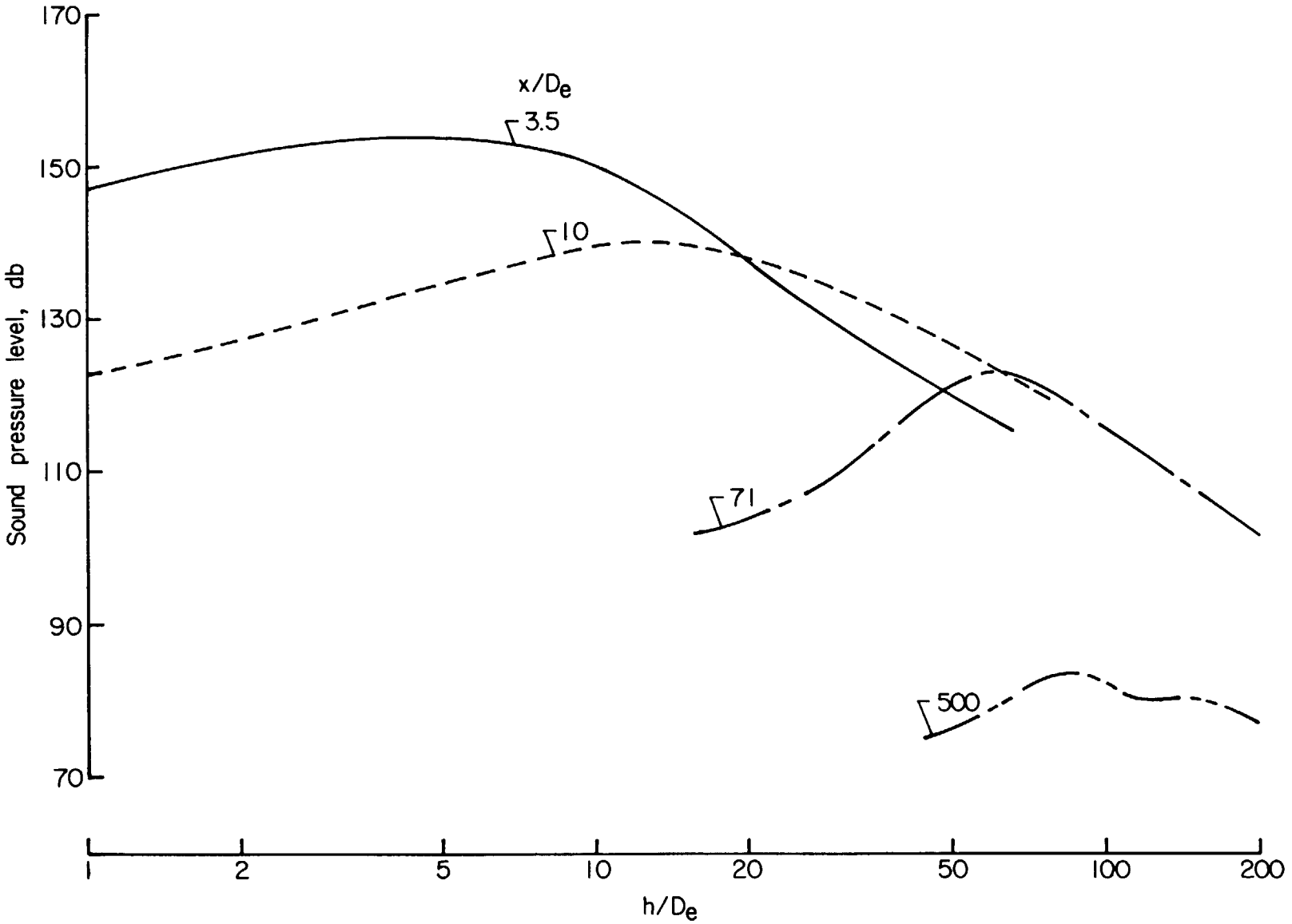

(h) 2,400 to 4,800 cps.

Figure 15.- Continued.

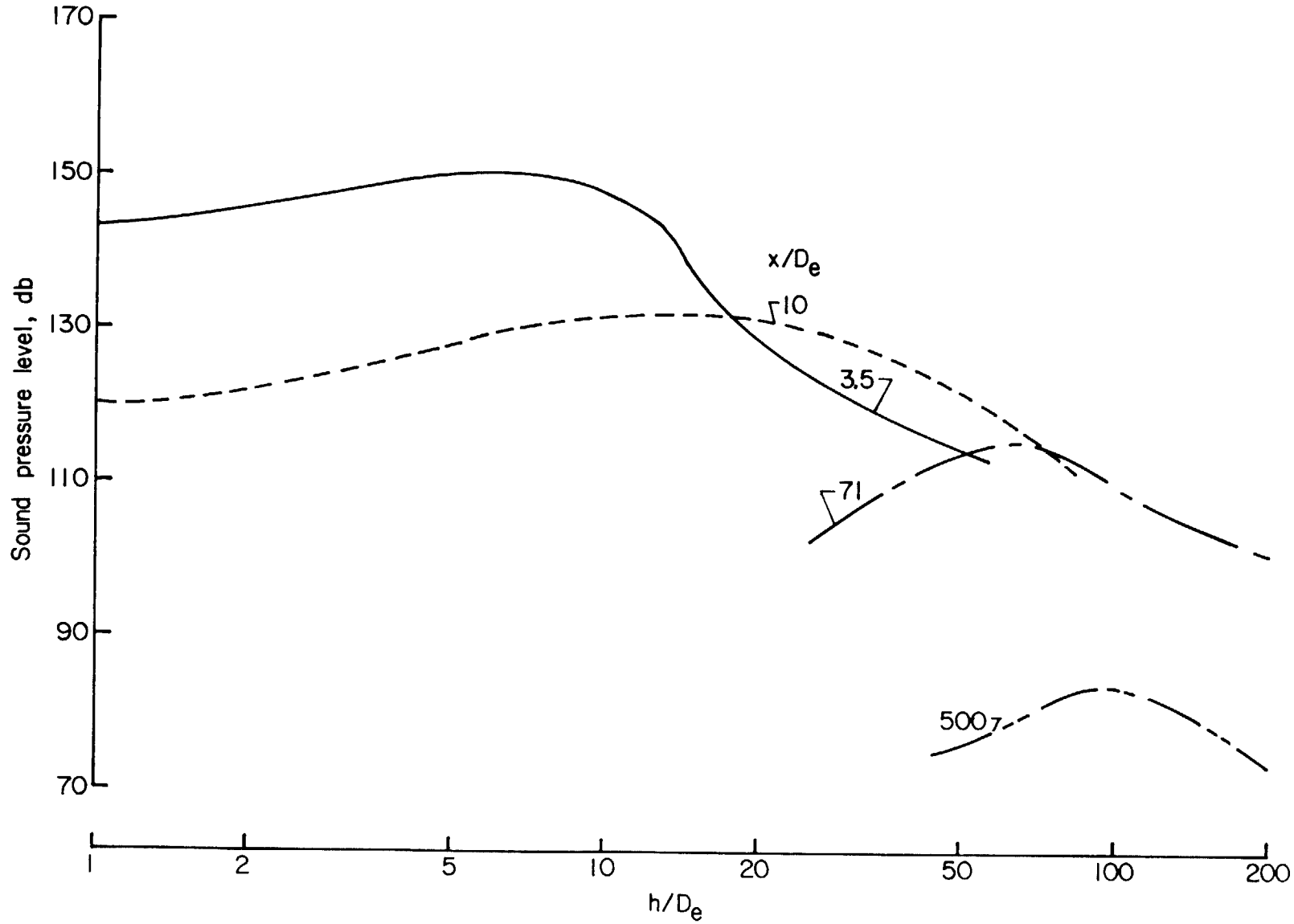

(i) 4,800 to 10,000 cps.

Figure 15.- Concluded.

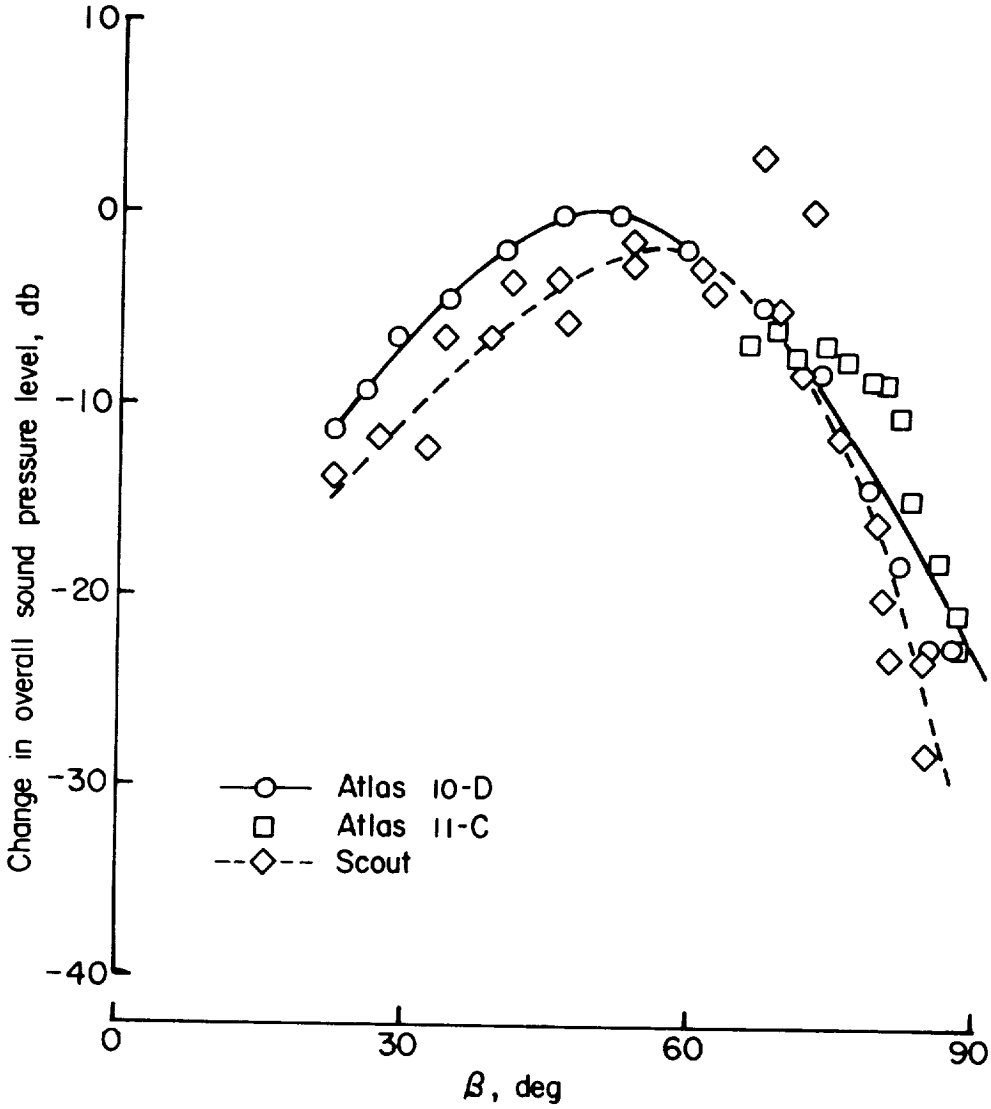

Figure 16.- Comparison of overall sound pressure levels as a function of azimuth angle β for Atlas and Scout launch vehicles at comparable operating conditions. 0 db on vertical scale corresponds to 134 db for the Atlas 10-D at a distance of 100 feet.